

Symbolic Side-Channel Analysis for Probabilistic Programs

Pasquale Malacaria*, MHR. Khouzani*, Corina S. Păsăreanu†, Quoc-Sang Phan‡, Kasper Luckow§

*Queen Mary University of London, London E1 4NS, UK

†Carnegie Mellon University and NASA Ames Research Center, Moffett Field, CA 94035, USA

‡Fujitsu Laboratories of America, Sunnyvale, CA 94085, USA

§Amazon Web Services, Cupertino, CA 95014, USA

Abstract—In this paper we describe symbolic side-channel analysis techniques for detecting and quantifying information leakage, given in terms of Shannon and Min Entropy. Measuring the precise leakage is challenging due to the randomness and noise often present in program executions and side-channel observations. We account for this noise by introducing additional (symbolic) program inputs which are interpreted probabilistically, using symbolic execution with parameterized model counting. We also explore an approximate sampling approach for increased scalability. In contrast to typical Monte Carlo techniques, our approach works by sampling symbolic paths, representing multiple concrete paths, and uses pruning to accelerate computation and guarantee convergence to the optimal results. The key novelty of our approach is to provide bounds on the leakage that are provably under- and over-approximating the real leakage. We implemented the techniques in the Symbolic PathFinder tool and we demonstrate them on Java programs.

1. Introduction

Pervasive proliferation of computer systems has increased access to sensitive information, ranging from financial and medical records of individuals to trade and military secrets of corporations or countries. It has become critical to develop tools and techniques to ensure that software systems that manipulate sensitive data do so in a secure manner. The confidentiality of secret data is particularly hard to achieve if an attacker can observe non-functional characteristics of a program behavior, for instance by measuring execution times or memory usage. Side-channel attacks [8], [9], [21], [25] aim to recover secret program data based on this kind of observations. Side-channel attacks are of grave concern and they have been shown to pose serious security threats. For instance, they can recover cryptographic keys from well-known encryption/decryption algorithms [8] or derive user-sensitive data from common compression algorithms [21].

In this paper we describe symbolic analysis techniques for quantifying information leaks in side channels. A key obstacle in reasoning about side-channel attacks is the randomness and noise that are often present in program executions and side-channel measurements. This can come from “outside” the program, due to measurements made

on noisy hardware platforms or over busy networks, but can also come from “inside” the program, due to explicit calls to Random methods in implementations of randomized algorithms (that are often used in security applications), or due to the thread scheduler or the garbage collector, which behave non-deterministically. Furthermore randomness can be introduced as a countermeasure against attacks, e.g. by adding random delays to a program to make it difficult for an adversary to infer secrets based on timing measurements. Thus, it is important to develop precise side channel analysis techniques to assess program leakage in the presence of random or noisy behavior and to determine if the implemented countermeasures are indeed effective.

To address this problem, we model both internal and external noise by creating additional (symbolic) inputs to the program. Conditions on these inputs are interpreted probabilistically using a probabilistic extension to symbolic execution [17]–[19]. The technique uses model counting over constraints collected with symbolic execution to compute probabilities of different program paths. In this paper, we adapt the technique to computing Shannon and Min-entropy leakage in the presence of internal and external randomness (or noise). We further describe optimizations based on *symbolic projection* [1] to avoid explicit enumeration over secret values. Our analysis is parametrized by an observation model which allows us to obtain the side-channel measurements from the execution of program instructions.

To address the potential scalability issues associated with symbolic execution and model counting, we also explore partial exploration techniques that sample the symbolic program space to gradually collect symbolic paths. In contrast to typical Monte Carlo approaches, the techniques sample over the *symbolic paths* which represent multiple concrete paths. Furthermore, each symbolic path needs to be sampled only once and is subsequently pruned, accelerating the analysis. Our key contribution is to provide concrete (non-probabilistic) *lower* and *upper bounds* on the information leakage, for Min-Entropy and Shannon-Entropy leakage, based on the partial exploration analysis. The computed bounds hold for any partial exploration (hence they are “any-time”), improve with more symbolic samples and are guaranteed to converge to the exact value of leakage.

There are few existing tools that can cope with noisy observations. Statistical analysis tools, such as LeakWatch [10], are often imprecise and require a huge number of samples. These tools run the program multiple times and use the outcome of each execution to get an estimate of the information channel (joint probabilities) and any function of it, specifically, leakage values. In contrast to our symbolic approach, statistical approaches have the advantage that they can be used in a “black-box” fashion, where no knowledge of the program or noise distribution is assumed. However, due to the random nature of sampling, the leakage values provided by statistical approaches are only approximate, with no guarantee that they over- or under- approximate the real leakage, which may lead to many false results (positive or negative). Furthermore the accuracy measures such as the confidence intervals provided by e.g. LeakWatch are still probabilistic, and to get a reliable value for them one often needs a large amount of samples. In contrast, our symbolic analysis technique is exact and our estimation approach reports bounds that are provably under- and over-estimating the real leakage, while avoiding resampling of the same (symbolic) path.

We have implemented the exact and partial symbolic analyses in the Symbolic PathFinder tool [38]. We illustrate them in the context of Java applications where we show how to obtain tight bounds on the leakage in the presence of internal and/or external randomness. Our approach can be easily adapted to work with other symbolic execution tools, targeting other programming languages.

Contributions and roadmap.

The main contributions of this work are:

- Introducing a symbolic execution framework for the analysis of side channels in probabilistic programs (Sections 4 and 5);
- Combining this symbolic execution analysis with Barvinok parametrized model counting to optimize the computation (Section 6);
- Developing a symbolic sampling approach to scale up the computation, and proving guarantees in terms of converging concrete upper and lower bounds, both for Shannon and Min-Entropy leakage, for our symbolic sampling algorithms (Section 7);
- Demonstrating the applicability of these techniques to challenging programs (provided by DARPA) and exhibiting the merits of our techniques compared with tools that use standard Monte Carlo techniques; we use “Leakwatch” [10] for comparison (Section 8).

2. Motivating Example

We illustrate our analysis with the example in Figure 1. Assume that the sensitive data h is uniformly distributed over the domain $\mathcal{D} = \{0, 1, 2\}$, that is:

$$p(h = 0) = p(h = 1) = p(h = 2) = \frac{1}{3}$$

The observable o , which can be for instance the execution time or the runtime power consumption, has three distinct values $obs1$, $obs2$, and $obs3$. The instance method `nextInt(2)` of `java.util.Random` also returns a uniformly distributed value from the set $\{0, 1\}$, and thus:

$$p(noise > 0) = p(\neg(noise > 0)) = \frac{1}{2}.$$

```
java.util.Random rg = new Random();
int noise = rg.nextInt(2);
if(noise > 0){
    if(h > 0)
        obs1;
    } else {
        obs2;
    }
} else{
    if(h > 1){
        obs1;
    } else {
        obs3;
    }
}
```

| | | $p(o, h)$ | | |
|-----|--------|-----------|--------|--------|
| h | $p(h)$ | $obs1$ | $obs2$ | $obs3$ |
| 0 | 1/3 | 0 | 1/6 | 1/6 |
| 1 | 1/3 | 1/6 | 0 | 1/6 |
| 2 | 1/3 | 1/3 | 0 | 0 |
| | $p(o)$ | 1/2 | 1/6 | 1/3 |

Figure 1: An example Java program and its corresponding joint probability matrix for (h, o) .

From the probability distribution of h and $noise$, constructing the joint probability matrix for (h, o) as in Figure 1 is straightforward. For example $(h = 0, o = obs1)$ cannot happen, so its probability is 0; $(h = 1, o = obs1)$ can only happen when $h = 1$ and $noise > 0$, hence its probability is $p(h = 1) \cdot p(noise > 0) = 1/3 \cdot 1/2 = 1/6$; $p(h = 2, o = obs1) = p(h = 2) = 1/3$ because when $h = 2$ the observable is $obs1$ regardless of the noise.

An adversary can learn something about the secret h by observing o . From this joint probability matrix, one can quantify this leakage using security metrics such as Shannon entropy or (Rényi’s) Min-Entropy, as we will overview later.

3. Background: Symbolic Execution and Parametrized Model Counting

To analyze side channels, we use symbolic execution [23]. Symbolic execution is a well known program analysis technique that executes programs on symbolic inputs, representing multiple concrete inputs, and computes the effects of the program as symbolic expressions over the inputs. The result of the analysis is a set of symbolic paths, each with a path condition PC , which is a conjunction of constraints characterizing the inputs that follow that path. Path conditions are checked for satisfiability with off-the-shelf solvers such as Z3 [13] to ensure the symbolic execution follows only feasible paths. To deal with loops and recursion, typically a bound is put on the exploration depth.

We use parameterized model counting, specifically “Barvinok” [1], for computing the leakage of noisy side channels efficiently. Barvinok [1] provides an efficient

procedure for model counting over linear integer arithmetic (LIA) constraints. A LIA constraint defines a multi-dimensional lattice bounded by a convex polytope [12]. The complexity of the algorithm does not depend on the actual size of the variable domains, making it suitable for the analysis of real programs (albeit limited to linear constraints).

In particular, we use Barvinok's `card` operation which computes the number of elements in a set, or the number of elements in the image of a domain element of a map [1, p.12]. The operation is performed exactly and symbolically and the result is a piecewise quasipolynomial, i.e., a subdivision of one or more spaces, with a quasipolynomial associated to each cell in the subdivision.

4. Analysis of Noisy Side Channels

Let $P(h)$ denote a program, where h is a high input (secret value) taken from the set \mathcal{D} . In this paper, we assume the high input (secret) is chosen uniformly from its space. We also assume that the public program inputs are fixed and can be hence treated as constants. Relaxing these two assumptions is left for future work.

Assuming a uniform distribution over the high values is compatible with practical situations, especially, in the context of cryptographic protocols, where the high value is the secret key. Also, if the distribution of the high can be selected, then it should be generally picked to be uniform, in order to maximize the uncertainty of an adversary. If the distribution cannot be picked, then the worst case for leakage (which pertains to "channel capacity") is still uniform distribution for the Min-Entropy leakage (though not for Shannon entropy).

Suppose an attacker tries to infer some information on the hidden secret h based on side channel measurements obtained when running the program. We assume that the attacker has full knowledge about the implementation of P . This assumption is justified as our goal is to give bounds on what side-channel attackers can, in principle, achieve.

Our setting is standard information theory [11]. With a slight abuse of notation, we use h and o to denote both the program secrets/output and the random variables representing them. For simplicity of presentation, we assume we have only one secret input; however all our results generalize to vectors of secrets in a straightforward way.

We compute the information *leakage*, i.e. number of bits in the secret leaked, based on Shannon's Information theory where the *observables* are the measurements computed for each path in the program. Let $\mathcal{O} = \{o_1, o_2, \dots, o_m\}$ denote the side-channel observations. Our analysis is parametrized by an *observation* function that gives these measurements for different kinds of side channels, e.g. execution time, number of bytes allocated, number of packets sent over a network, etc.

By definition, when considering systems whose only input is a confidential value h , leakage is the *mutual information* between the observable and the secret [30]:

$$\text{Leakage}^S = \mathcal{I}(h; o) = \mathcal{H}(o) - \mathcal{H}(o|h), \quad (1)$$

where $\mathcal{H}(X)$ is classical Shannon entropy, measuring "uncertainty" about a random variable X . Let $p(o_i)$ be the probability of observing o_i (i.e. side-channel measurement in our case). Then, Shannon's entropy is defined as:

$$\mathcal{H}(o) = - \sum_{o_i \in \mathcal{O}} p(o_i) \log_2 p(o_i).$$

The second term in (1) is the conditional entropy of the observable given the input and is computed as follows:

$$\mathcal{H}(o|h) = \sum_{h_j \in \mathcal{D}} p(h_j) \mathcal{H}(o|h_j),$$

where $\mathcal{H}(o|h_j)$ is the Shannon entropy computed for the conditional probability of $p(o|h_j)$. $\mathcal{H}(o|h)$ can be thought of as the amount of uncertainty about the observable as the effect of noise, and we will hence refer to it as "entropy of noise". If we consider a deterministic system and without any noise then $\mathcal{H}(o|h) = 0$ since there is no uncertainty about the observable when the inputs are given. Thus the leakage is simply $\mathcal{H}(o)$. In the presence of noise, probabilistic scheduler, or garbage collection, $\mathcal{H}(o|h) > 0$, so the leakage is smaller.

Note that there are several equivalent ways to compute the leakage defined as Shannon mutual information. Namely:

$$\begin{aligned} \text{Leakage}^S &= \mathcal{I}(h; o) = \mathcal{H}(o) - \mathcal{H}(o|h) = \\ &\mathcal{H}(o) + \mathcal{H}(h) - \mathcal{H}(h, o) = \mathcal{H}(h) - \mathcal{H}(h|o). \end{aligned}$$

where $\mathcal{H}(h, o)$ is the "joint" entropy of random variables h , o , given as: $\mathcal{H}(h, o) = - \sum_{i,j} p(h_j, o_i) \log_2 p(h_j, o_i)$.

Noise can come from "outside" the program, e.g. due to measurements made on a noisy hardware platform or over a busy network, but can also come from "inside" the program, e.g. due to explicit calls to `java.util.Random` methods. Further, noise can be due to the thread scheduler or the garbage collector, which behave non-deterministically. In this paper we "internalize" all these different kinds of noise. We introduce an additional input (or inputs) "noise", denoted by n , and we compute leakage of noisy programs $P(h)$ by analyzing programs of the form $P(h, n)$, using probabilistic symbolic execution [5], [17]. As we shall see, the analysis needs to be performed with care, and treats these inputs differently when computing the conditional entropy.

As an example, consider again the code in Figure 1. We replace variable `noise` with an additional input with appropriate range (0..1 in this case) such that the probability of executing each branch of the condition involving this input is 50%, assuming a uniform input distribution. Similarly, for a multi-threaded program, we introduce symbolic inputs with appropriate ranges and conditions that execute with each context switch. Furthermore, noise in external measurements (e.g. made over a busy network) can be modeled by adding symbolic inputs and extra conditions that execute at the end of each program path. For the purposes of this paper, we assume that the operation modeling the probabilistic noise is given. In practice, this can be a challenging task requiring

side information and extensive profiling of the system; this topic is, however, orthogonal to this work.

4.1. Min-Entropy

We also consider the leakage expressed as *Min-Entropy* [40]. Min-Entropy leakage measures how much the observations increase the probability of guessing the secret in one try. Researchers have argued that to reason in terms of probability of guessing the secret is in many cases more natural and appropriate when quantifying leakage.

The leakage expressed as Min-Entropy (which we will refer to as Min-leakage) is as follows:

$$\text{Leakage}^M = \log_2 \left(\frac{\sum_i \max_j p(h_j, o_i)}{\max_j p(h_j)} \right). \quad (2)$$

As a simple example justifying Min-Entropy consider the following probability distributions over the secret:

$$p_1 = (1/2, 1/2), \quad p_2 = (1/2, 1/2^{1000}, \dots, 1/2^{1000}).$$

These distributions have very different Shannon entropies (for p_1 , it is 1 bit, while for p_2 , it is 500.5 bits). However, they have the same Min-Entropy which capture that with probability 1/2 the best guess is correct.

Thus, when considering both Shannon and Min Entropy formulation of leakage, we seek to perform an efficient computation of the “joint” probabilities, and this will be one of the main objective of our algorithms.

4.2. Observation models

The analysis is parametrized by an observation model, which provides measurements for the following:

- *execution time*: based on a model which maps each bytecode instruction to a timing observation, the execution time of a symbolic path is computed as the sum of timing observations of all instructions along the path.
- *memory usage*: by monitoring the Java Bytecode instructions that allocate memory (e.g., NEW and NEWARRAY) we can compute the number of heap objects allocated along a symbolic path. Further we compute the memory allocated for live heap objects along a path.
- *network and file communication*: the observable is the number of bytes written to a TCP socket or a file. In both cases, the writing is done via multiple invocations of the method `write` of `java.io.OutputStream`, which writes 1 byte to the stream. The listener monitors the bytecode instruction `INVOKEVIRTUAL` to check how many times `write` is called.

For cases that do not fall into the categories above, we developed another listener that monitors user-defined observables. A precise model for e.g. timing measurements needs to take into account low-level features of the target platform including processor architecture, pipelining, and branch prediction. For this paper, we assume that the observation model is given and consider building precise models

out-of-scope. Furthermore we do not consider cache side channels primarily because they are out of scope for our Java project. However the tool that we use does have its own memory model that could be adapted for considering cache effects.

5. Computing Leakage via Symbolic Execution

In this section, we will show how to use the formula $\text{Leakage}^S = \mathcal{H}(o) - \mathcal{H}(o|h)$ to compute the leakage using symbolic execution and model counting. We will first compute $\mathcal{H}(o)$ by computing $p(o)$ ’s and then $\mathcal{H}(o|h)$ by computing $p(o|h)$ for each high input. Later in this paper we will optimize this process by providing a completely symbolic approach.

We compute $\mathcal{H}(o)$ using symbolic execution and model counting adapting the procedure from previous work that studies noiseless side channels [37]. Specifically we assume that the program under analysis is modified to explicitly add the noise as an extra input. We perform a symbolic execution over the program $P(h, n)$ where we set the secret and noise inputs to fresh symbolic values (the inputs can be vectors) ranging over possibly very large but finite domains. We further assume that there are no infinite loops (loops with symbolic conditions will terminate due to the finite domain assumption).

The result of symbolic execution is a finite set of (feasible) symbolic paths $\pi_1, \pi_2, \dots, \pi_n$ each with a path condition $(PC_1, PC_2, \dots, PC_n)$. Let $\text{obs}(\pi_i)$ represent the side-channel measurement along that path according to the observation function. Thus we assume that each symbolic path can give only one observable, but different paths can give the same observable. Our work is done in the context of a project that specifically targets side channels for Java programs but our work is applicable to other types of quantitative flow analysis where this assumption holds. To simplify the notation, we write $\text{obs}(PC_i)$ to mean $\text{obs}(\pi_i)$.

We group the path conditions that lead to same observation o_i into *clauses*, i.e. $C_i \equiv \bigvee_{\text{obs}(PC_j)=o_i} PC_j$. Each clause characterizes the set of secret and noise values that lead to the same observation. The procedure called **ComputeConstraints** is described below.

Procedure: ComputeConstraints($P(h, n)$, $\text{obs}(\cdot)$)

- 1 $\mathcal{O} \leftarrow \emptyset, \mathcal{C} \leftarrow \emptyset$
 - 2 $\mathcal{PC} \leftarrow \text{SymbolicExecution}(P(h, n))$
 - 3 **foreach** $PC \in \mathcal{PC}$ **do**
 - 4 $\mathcal{O} \leftarrow \mathcal{O} \cup \{\text{obs}(PC)\}$
 - 5 **foreach** $o_i \in \mathcal{O}$ **do**
 - 6 $C_i \leftarrow \bigvee_{\text{obs}(PC_j)=o_i} PC_j$
 - 7 **return** \mathcal{C}
-

Furthermore we compute $\mathcal{H}(o)$ by applying a model counting procedure over the clauses to calculate the proba-

bilities for each observation. Assuming a uniform distribution over the secret, the probability of observing o_i is:

$$p(o_i) = \frac{\#(C_i)}{|\mathcal{D}| \cdot |\mathcal{D}_n|} = \frac{\sum_{\text{obs}(PC_j)=o_i} \#(PC_j)}{|\mathcal{D}| \cdot |\mathcal{D}_n|}.$$

Here $\#(c)$ denotes the number of solutions, i.e. possible values satisfying the constraint c , assuming that the secret and the noise values range over domains \mathcal{D} and \mathcal{D}_n , respectively. This count can be computed with an off-the-shelf model-counting procedure such as Barvinok [1]. We use $|\mathcal{D}|$ and $|\mathcal{D}_n|$ to denote the size of the secret and noise domains respectively. They can be large but finite. The procedure, called **entropyObs**, is illustrated below.

Procedure: entropyObs($P(h, n)$, $\text{obs}(\cdot)$)

```

1  $\mathcal{C} \leftarrow \text{ComputeConstraints}(P(h, n), \text{obs}(\cdot))$ 
2 foreach  $C_i \in \mathcal{C}$  do
3    $\mathcal{H}_o \leftarrow 0$ 
4    $p(o_i) = \frac{\#(C_i)}{|\mathcal{D}| \cdot |\mathcal{D}_n|} = \frac{\sum_{\text{obs}(PC_j)=o_i} \#(PC_j)}{|\mathcal{D}| \cdot |\mathcal{D}_n|}$ 
5    $\mathcal{H}_o \leftarrow \mathcal{H}_o - p(o_i) \log_2(p(o_i))$ 
6 return  $\mathcal{H}_o$ 

```

For the computation of $\mathcal{H}(o|h)$ the simplest approach, but always doable, is to iterate over each concrete value h_j of h and compute the entropy $\mathcal{H}(o|h_j)$ as the entropy of the observable, using the procedure described above. The only difference is that now we perform Symbolic Execution over the program using the concrete value h_j , but noise is still symbolic. Finally, since we assume uniform distribution for h , we have $p(h_j) = \frac{1}{|\mathcal{D}|}$, and hence:

$$\mathcal{H}(o|h) = \sum_{h_j \in \mathcal{D}} p(h_j) \mathcal{H}(o|h_j) = \frac{1}{|\mathcal{D}|} \sum_{h_j \in \mathcal{D}} \mathcal{H}(o|h_j).$$

The overall procedure for computing the leakage in the presence of noise is given in Algorithm 1.

Algorithm 1: Shannon leakage of noisy side channels

```

1  $h \leftarrow \text{makeSymbolic}'(h')$ 
2  $n \leftarrow \text{makeSymbolic}'(n')$ 
3  $\mathcal{H}_o \leftarrow \text{entropyObs}(P(h, n), \text{obs}(\cdot))$ 
4  $\mathcal{H}_{o|h} \leftarrow 0$ 
5 foreach  $h_j \in \mathcal{D}$  do
6    $\mathcal{H}_{o|h} \leftarrow \mathcal{H}_{o|h} + \text{entropyObs}(P(h_j, n), \text{obs}(\cdot))$ 
7    $\mathcal{H}_{o|h} \leftarrow \frac{1}{|\mathcal{D}|} \cdot \mathcal{H}_n$ 
8    $\text{Leakage}^S \leftarrow \mathcal{H}_o - \mathcal{H}_{o|h}$ 
9 return  $\text{Leakage}^S$ 

```

Note that in practice, we do not need to perform repeated symbolic execution for each value h_j of the secret. Instead

we can invoke symbolic execution once and instantiate the symbolic path conditions for the different values of h . Furthermore, the computation can be made efficient as we only need to compute the entropy of noise along the paths that are conditioned on noise; all the other paths have no uncertainty and can thus be ignored.

Similarly, Algorithm 2 computes Min-entropy leakage as defined in (2) using symbolic execution. In particular, the notation $\#(C_i(h_j))$ designates the number of solutions for noise that satisfy the clause C_i for a given h_j .

Algorithm 2: Minleakage of noisy side channels

```

1  $h \leftarrow \text{makeSymbolic}'(h')$ 
2  $n \leftarrow \text{makeSymbolic}'(n')$ 
3  $\mathcal{C} \leftarrow \text{ComputeConstraints}(P(h, n), \text{obs}(\cdot))$ 
4  $\text{prob} \leftarrow 0$ 
5 foreach  $C_i \in \mathcal{C}$  do
6    $\text{max} \leftarrow 0$ 
7   foreach  $h_j \in \mathcal{D}$  do
8      $p(o_i, h_j) \leftarrow \frac{\#(C_i(h_j))}{|\mathcal{D}| \cdot |\mathcal{D}_n|}$ 
9     if  $\text{max} < p(o_i, h_j)$  then
10        $\text{max} \leftarrow p(o_i, h_j)$ 
11    $\text{prob} \leftarrow \text{prob} + \text{max}$ 
12  $\text{Leakage}^M \leftarrow \log_2(\text{prob} \cdot |\mathcal{D}|)$ 
13 return  $\text{Leakage}^M$ 

```

Example. Consider the example introduced in Section 2. Running symbolic execution over the program (where both h and noise n are symbolic) results in four paths but only in three observables, since two paths lead to the same observation. As mentioned, we group the path conditions for the paths that lead to the same observation into a clause and we apply model counting over the clauses.

$$\begin{aligned} p(\text{obs1}) &= \frac{\#(n > 0 \wedge h > 0) + \#(n \leq 0 \wedge h > 1)}{|\mathcal{D}| \cdot |\mathcal{D}_n|} \\ &= \frac{|\{1, 2\}| \cdot \#(n > 0) + |\{2\}| \cdot \#(n \leq 0)}{|\mathcal{D}| \cdot |\mathcal{D}_n|} = \frac{2 \cdot 1 + 1 \cdot 1}{3 \cdot 2} = \frac{1}{2} \\ p(\text{obs2}) &= \frac{\#(n > 0 \wedge h \leq 0)}{|\mathcal{D}| \cdot |\mathcal{D}_n|} = \frac{|\{0\}|}{3} \cdot \frac{\#(n > 0)}{|\mathcal{D}_n|} = \frac{1}{3} \cdot \frac{1}{2} = \frac{1}{6} \\ p(\text{obs3}) &= \frac{\#(n \leq 0 \wedge h \leq 1)}{|\mathcal{D}| \cdot |\mathcal{D}_n|} = \frac{|\{0, 1\}|}{3} \cdot \frac{\#(n \leq 0)}{|\mathcal{D}_n|} = \frac{2}{3} \cdot \frac{1}{2} = \frac{1}{3} \\ \Rightarrow \mathcal{H}(o) &= -\frac{1}{2} \log_2\left(\frac{1}{2}\right) - \frac{1}{3} \log_2\left(\frac{1}{3}\right) - \frac{1}{6} \log_2\left(\frac{1}{6}\right) = 1.459148 \text{ bits} \end{aligned}$$

On the other hand:

$$\mathcal{H}(o|h) = \frac{1}{3} (\mathcal{H}(o|h=0) + \mathcal{H}(o|h=1) + \mathcal{H}(o|h=2)).$$

When $h = 0$, there are two observables obs2 and obs3 with the same probability $\frac{1}{2}$. Therefore $\mathcal{H}(o|h=0) = 1$. When $h = 1$, there are two observables obs1 and obs3 with the same probability $\frac{1}{2}$. Therefore $\mathcal{H}(o|h=1) = 1$. When $h = 2$, there is only one observable obs1 with probability 1. Therefore $\mathcal{H}(o|h=2) = 0$. Hence:

$$\Rightarrow \text{Leakage}^S = 1.459148 - \frac{2}{3} = 0.7924813 \text{ bits}$$

6. Optimised Computation of Leakage

In the previous section we described an algorithm for computing the entropy of noise and hence the leakage by enumerating over all the values of the secret, and computing $\mathcal{H}(o|h_j)$ for each one of the high values, using symbolic execution and model counting. However this can be expensive since the domain of h , \mathcal{D} , can be very large. In this section we explore optimizations based on Barvinoks parametrized model counting procedure [1] to optimize this computation.

Let us revisit the computation of the noise:

$$\mathcal{H}(o|h) = \mathcal{H}(h, o) - \mathcal{H}(h),$$

where $\mathcal{H}(h, o)$ is the joint entropy of h, o , and is computed as follows:

$$\mathcal{H}(h, o) = - \sum_{i,j} p(h_j, o_i) \log_2 p(h_j, o_i).$$

Using symbolic execution and model counting, it can be computed as:

$$\mathcal{H}(h, o) = - \sum_i \sum_j \frac{\#(C_i \wedge h = h_j)}{|\mathcal{D}| \cdot |\mathcal{D}_n|} \cdot \log_2 \frac{\#(C_i \wedge h = h_j)}{|\mathcal{D}| \cdot |\mathcal{D}_n|}.$$

Recall that clause C_i is the disjunction of all the path conditions that lead to the same observation o_i . Note that the entropy of the secret $\mathcal{H}(h)$ is simply $\log_2 |\mathcal{D}|$.

For a clause C_i we propose to use Barvinok [1] to *decompose* the cardinality of the solution set for C_i into its projections on the values of high input h and noise n . As we will demonstrate, this decomposition is useful for obtaining efficient computations of the leakage.

To illustrate Barvinok's functionality, consider the following example, where a clause C is $(n > 0 \wedge h > 0) \vee (n \leq 0 \wedge h > 1)$, and the domains for n and h are $[0 \dots 2]$ and $[0 \dots 1000000]$ respectively. The result returned automatically by Barvinok is a function F_C as follows:

$$F_C(h) = \begin{cases} 2 & \text{if } h = 1 \\ 3 & \text{if } 2 \leq h \leq 1000000 \end{cases}$$

The result can be interpreted as follows. Given a choice for h , the number of solutions for C is $F_C(h)$. Thus, if $h = 1$, clause C has $F_C(1) = 2$ solutions. This is easy to verify since when $h = 1$ clause C becomes $(n > 0 \wedge 1 > 0) \vee (n \leq 0 \wedge 1 > 1)$ which simplifies to $(n > 0)$, which has 2 solutions. On the other hand, if $h = 2$, clause C has $F_C(2) = 3$ solutions. In fact, for any value of h such that $2 \leq h \leq 1000000$, there are three solutions satisfying C . Again this is easy to verify. For example, if $h = 2$, clause C becomes $(n > 0 \wedge 2 > 0) \vee (n \leq 0 \wedge 2 > 1)$ which simplifies to $(n > 0 \vee n \leq 0)$ which is satisfied by any value of noise. Another observation is that F_C gives the number of *noise* values that satisfy C for a particular value of h . Thus F_C can be seen as the decomposition of the solution space for $\#C$ with respect to h and n .

More generally, for any clause C_i we can use Barvinok's card operation to obtain a counting function $F_{C_i} : \mathcal{D} \rightarrow \mathbb{N}$,

such that $F_{C_i}(h_j)$ gives the number of solutions for $(C_i \wedge h = h_j)$. We can then compute the joint entropy as follows.

$$\textbf{Proposition 1. } \mathcal{H}(h, o) = - \sum_i \sum_j \frac{F_{C_i}(h_j)}{|\mathcal{D}| \cdot |\mathcal{D}_n|} \cdot \log_2 \frac{F_{C_i}(h_j)}{|\mathcal{D}| \cdot |\mathcal{D}_n|}.$$

Thus, when computing the entropy of noise, we can use function application (of F_{C_i}) which is more efficient than the repeated invocation of a model counting procedure for computing $\#(C_i \wedge h = h_j)$ for all the values h_j in \mathcal{D} .

6.1. Separable constraints

The computation of leakage based on Shannon entropy can be made more efficient for an interesting special case where the constraints on noise n and high input h are *separable*. That is, each path condition PC can be written as $\phi_n \wedge \phi_h$, i.e., as a conjunction of constraints ϕ_n and ϕ_h , where ϕ_n is a constraint on noise variable and ϕ_h is a constraint on the secret. In other words, in such cases, the noise variables are not directly compared to secret values; this is a common case for noise that models multi-threading, imprecisions in hardware side-channel measurements, or defense mechanisms that add some noise to programs' computations. Consider our running example from Section 2. Recall PC_1 is $n > 0 \wedge h > 0$. Thus $\phi_n = (n > 0)$ and $\phi_h = (h > 0)$.

For such cases, Barvinok's card operation generates a counting function of the following form:

$$F_{C_i}(h) = \begin{cases} N_{1,n}^i & h \models c_{1,h}^i \\ N_{2,n}^i & h \models c_{2,h}^i \\ \vdots & \\ N_{m,n}^i & h \models c_{m,h}^i \end{cases} \quad (3)$$

Here function F_{C_i} decomposes the solution space of $\#C_i$ in m components: for each component, the number of solutions is a *constant* number, denoted $N_{k,n}^i$ (for $k = 1, \dots, m$), when the secret h satisfies the corresponding condition, denoted $c_{k,h}^i$. The function $F_{C_i}(h)$ can be compactly represented by the set of pairs of $\langle N_{k,n}^i, c_{k,h}^i \rangle$ for $k = 1, \dots, m$. By construction, we have the following.

$$\#C_i = \sum_{k=1}^m N_{k,n}^i \cdot \#c_{k,h}^i.$$

Note that all $c_{k,h}^i$ are disjoint and their union defines all the h values that satisfy C_i ; thus the conditions $c_{k,h}^i$ define a partition over the secrets satisfying C_i . We use these properties below.

First note that $\#(C_i \wedge h = h_j) = N_{k,n}^i$ if h_j is a solution to C_i (and further it is a solution of $c_{k,h}^i$), since the projection on h should have exactly one value, i.e. h_j , and it is 0 if h_j is not a solution to C_i . Further, the number of times $\#(C_i \wedge h = h_j) = N_{k,n}^i$ is exactly $\#c_{k,h}^i$. Thus

we can use the piecewise decomposition for clause C_i to perform the following simplifications:

$$\begin{aligned} \sum_j \frac{\#(C_i \wedge h = h_j)}{|\mathcal{D}| \cdot |\mathcal{D}_n|} \cdot \log_2 \frac{\#(C_i \wedge h = h_j)}{|\mathcal{D}| \cdot |\mathcal{D}_n|} &= \\ \sum_{h \models c_{1,h}^i} \frac{N_{1,n}^i}{|\mathcal{D}| \cdot |\mathcal{D}_n|} \cdot \log_2 \frac{N_{1,n}^i}{|\mathcal{D}| \cdot |\mathcal{D}_n|} & \\ + \sum_{h \models c_{2,h}^i} \frac{N_{2,n}^i}{|\mathcal{D}| \cdot |\mathcal{D}_n|} \cdot \log_2 \frac{N_{2,n}^i}{|\mathcal{D}| \cdot |\mathcal{D}_n|} & \\ + \dots & \\ + \sum_{h \models c_{m,h}^i} \frac{N_{m,n}^i}{|\mathcal{D}| \cdot |\mathcal{D}_n|} \cdot \log_2 \frac{N_{m,n}^i}{|\mathcal{D}| \cdot |\mathcal{D}_n|} & \\ = \sum_{k=1}^m \#c_{k,h}^i \cdot \frac{N_{k,n}^i}{|\mathcal{D}| \cdot |\mathcal{D}_n|} \cdot \log_2 \frac{N_{k,n}^i}{|\mathcal{D}| \cdot |\mathcal{D}_n|}. & \end{aligned}$$

Thus, instead of iterating over all possible values of h (with index j) we only need to iterate over the partitions over h (with index k) as computed symbolically by Barvinok. It follows that:

Proposition 2.

$$\mathcal{H}(h, o) = - \sum_i \sum_k \#c_{k,h}^i \cdot \frac{N_{k,n}^i}{|\mathcal{D}| \cdot |\mathcal{D}_n|} \cdot \log_2 \frac{N_{k,n}^i}{|\mathcal{D}| \cdot |\mathcal{D}_n|}.$$

Thus,

$$\begin{aligned} \mathcal{H}(o|h) &= - \sum_{i,k} \#c_{k,h}^i \cdot \frac{N_{k,n}^i}{|\mathcal{D}| \cdot |\mathcal{D}_n|} \cdot \log_2 \frac{N_{k,n}^i}{|\mathcal{D}| \cdot |\mathcal{D}_n|} - \log_2 |\mathcal{D}| \\ &= - \sum_{i,k} \#c_{k,h}^i \cdot \frac{N_{k,n}^i}{|\mathcal{D}| \cdot |\mathcal{D}_n|} \cdot \log_2 \frac{N_{k,n}^i}{|\mathcal{D}_n|}. \end{aligned}$$

Algorithm 3 shows the optimized way to compute the Shannon leakage based on the above proposition.

Algorithm 3: OptimizedLeakage

```

1  $h \leftarrow makeSymbolic('h')$ 
2  $\mathcal{C} \leftarrow \text{ComputeConstraints}(P(h, n), \text{obs}(\cdot))$ 
3  $\mathcal{H}_o \leftarrow \text{entropyObs}(P(h, n), \text{obs}(\cdot))$ 
4  $\mathcal{H}_{o|h} \leftarrow 0$ 
5 foreach  $C_i \in \mathcal{C}$  do
6    $\mathcal{S}_i \leftarrow BarvH(C_i)$  /* BarvH: Barvinok
      'card' operation,  $F_{C_i}(h)$ , as in (3) */
7   foreach  $\langle N_j, c_j \rangle \in \mathcal{S}_i$  do
8     if  $max < \frac{N_j}{|\mathcal{D}| \cdot |\mathcal{D}_n|}$  then
9        $max \leftarrow \frac{N_j}{|\mathcal{D}| \cdot |\mathcal{D}_n|}$ 
10   $prob \leftarrow prob + max$ 
11  $Leakage^S \leftarrow \mathcal{H}_o - \mathcal{H}_{o|h}$ 
12 return  $Leakage^S$ 

```

Example. Consider again our running example. Recall that there are for path conditions that lead to three observations. We therefore have three clauses:

$$\begin{aligned} C_1 &:= (h > 0 \wedge n > 0) \vee (h > 1 \wedge n \leq 0) \\ C_2 &:= h \leq 0 \wedge n > 0 \\ C_3 &:= h \leq 1 \wedge n \leq 0 \end{aligned}$$

Running Barvinok on the three clauses gives the following:

$$\begin{aligned} F_{C_1}(h) &= \begin{cases} 2, & h = 2 \\ 1, & h = 1 \end{cases} \\ F_{C_2}(h) &= 1, h = 0 \\ F_{C_3}(h) &= 1, 0 \leq h \leq 1 \end{aligned}$$

Using our notations, $\mathcal{S}_1 = \{\langle 2, h = 2 \rangle, \langle 1, h = 1 \rangle\}$ etc. Thus, $\mathcal{H}(o|h) = -1 \cdot 2/6 \cdot \log_2 2/6 - 1 \cdot 1/6 \cdot \log_2 1/6 - 1 \cdot 1/6 \cdot \log_2 1/6 - 2 \cdot 1/6 \cdot \log_2 1/6 - \log_2 3 = 2/3$.

6.2. Computing Min-Entropy Leakage

Algorithm 4: Min-entropy Leakage

```

1  $h \leftarrow makeSymbolic('h')$ 
2  $\mathcal{C} \leftarrow \text{ComputeConstraint}(P(h, n), \text{obs}(\cdot))$ 
3  $prob \leftarrow 0$ 
4 foreach  $C_i \in \mathcal{C}$  do
5    $max \leftarrow 0$ 
6    $\mathcal{S}_i \leftarrow BarvH(C_i)$  /* BarvH: Barvinok
      'card' operation,  $F_{C_i}(h)$ , as in (3) */
7   foreach  $\langle N_j, c_j \rangle \in \mathcal{S}_i$  do
8     if  $max < \frac{N_j}{|\mathcal{D}| \cdot |\mathcal{D}_n|}$  then
9        $max \leftarrow \frac{N_j}{|\mathcal{D}| \cdot |\mathcal{D}_n|}$ 
10   $prob \leftarrow prob + max$ 
11  $Leakage^M \leftarrow \log_2(prob \cdot |\mathcal{D}|)$ 
12 return  $Leakage^M$ 

```

Algorithm 4 computes the min-leakage optimized by using the Barvinok decomposition. We compute the set of constraints, each one corresponds to an observable, similar to the previous sections. For each C_i we compute the maximal probability $\max_j p(h_j, o_i)$ as the following. We project C_i on h (line 6), decomposing the domain of h into partition, of which the equivalence relation \sim is defined as: $h_1 \sim h_2 \iff p(h_1, o_i) = p(h_2, o_i)$

Each block j in the partition is characterized by the pair $\langle s_j, c_j \rangle$ where s_j is the projection of C_i and s_j is the condition of h that satisfies the block. We iterate over the blocks of the partition (line 7 to line 9) to find the maximal probability for o_i . The rest is straightforward from the formula.

Thus, for our running example, we can compute $prob = 2/6 + 1/6 + 1/6 = 2/3$ giving Min-Entropy Leakage $\log_2(2/3 \cdot 3) = 1$.

6.3. Control-flow Side Channels

We discuss briefly an interesting special case where each observable is associated to a single path condition and the constraints on noise and secret are separable. This corresponds to the so called “control-flow side channels” [2], [35], [39]. In these cases the attacker can identify which path is executed by observing the trace of all program counter values, and more recently, also all memory location accessed during execution.

As before, we can decompose each path condition PC_i as: $\phi_n^i \wedge \phi_h^i$. Since ϕ_n and ϕ_h are separated, it follows that $\#PC_i = \#\phi_n^i \cdot \#\phi_h^i$. Hence:

$$p(o_i) = \frac{\#PC_i}{|\mathcal{D}| \cdot |\mathcal{D}_n|} = \frac{\#\phi_n^i \cdot \#\phi_h^i}{|\mathcal{D}| \cdot |\mathcal{D}_n|}.$$

We can use this observation and the calculations for $\mathcal{H}(o|h)$ from the previous sections to simplify the leakage formula in a way which is useful for symbolic computation.

Proposition 3. *When each observable is associated to a single path condition and the constraints on secret and noise are separable, we have:*

$$\text{Leakage}^S = - \sum_i p(o_i) \log_2 \frac{\#\phi_h^i}{|\mathcal{D}|}.$$

The algorithms for computing leakage for control-flow side channels are straightforward and are omitted for brevity.

6.4. Leakage Computation in the Presence of Both High and Low inputs

We now discuss the case when the program depends not only on the confidential input h but also on the public input l . In this case the leakage is defined using conditional mutual information [30], i.e.

$$\mathcal{I}(h; o|l) = \mathcal{H}(o|l) - \mathcal{H}(o|h, l)$$

again in the case of deterministic systems the term $\mathcal{H}(o|h, l)$ is 0 and the above reduces to $\mathcal{H}(o|l)$. When we fix a low input, it can be seen as a constant within the program, and we can then see the program as a system that is only dependent on the high input, for which we can use the leakage formulas we have presented in the previous sections.

We can also treat the public input l symbolically and apply parameterized model counting and numerical optimization to find the low value that maximizes the leakage, in a way similar to [36] (that work does not consider noise). However, the technical development of such an approach is beyond the scope of this paper, we leave its presentation for future work.

7. Symbolic Sampling With Path Pruning

The leakage computations that we have presented are computationally demanding as they involve exploring all the symbolic program paths (up to a user specified bound) and

performing expensive (parametrized) model counting over the collected path conditions. We describe here alternative *sampling techniques* to scale up the computation of leakage.

Instead of full, exhaustive symbolic execution, we perform sampling over the symbolic paths. The approach works as follows: A sample is obtained by performing one symbolic execution run; whenever a condition depending on a symbolic value is encountered, the decision of exploring either the *then* or the *else* branch is then determined randomly by breaking the tie arbitrarily, resulting in one symbolic path through the program.

Note that instead of doing pure Monte Carlo sampling as done in previous approaches [10], [20] we perform sampling over the *symbolic paths*. Each symbolic path represents multiple concrete paths all following the same control flow in the program. Thus, it is not necessary to sample along the same path multiple times, since repeated sampling can not bring new information to the analysis. We can therefore *prune* the explored paths, reducing the search space and accelerating the analysis.

The result of this analysis, after taking multiple samples, is a *subset* of the symbolic paths of the program, over which we can apply the leakage computation as described in the previous sections. Our goal is to compute *bounds (lower and upper bounds)* on the actual leakage of the program; we discuss the issue in more detail below. The approach that we propose is an *anytime* analysis that generally improves with more samples.

Since the analysis with pruning always explores new paths, and since we assume a finite number of paths, it follows that the search converges to an exhaustive analysis and that precise program leakage will be computed eventually.

Proposition 4 (Convergence of symbolic sampling with pruning). *If pruning is enabled, then all the symbolic program paths are guaranteed to be sampled yielding the precise leakage computation for the program.*

7.1. Anytime Bounds for Leakage

As we mentioned, even with symbolic execution and Barvinok counting, the process of computing leakage for a practical program can be long. Especially, each time a loop is encountered in the program, then it can be unwound a number of times during symbolic execution resulting in an impractical amount of paths to explore. Symbolic sampling with path-pruning will explore only a subset of the symbolic program paths, leading to partial learning of the (side-)channels of the program, which is guaranteed to eventually lead to full learning. In this section, we provide both upper and lower bounds (over and under-estimations) for the leakage given any partial learning of the channel. Both of the bounds monotonically converge to the actual value of leakage as more sample paths are examined. These bounds are “any-time” bounds, in the following sense: they are guaranteed that at any time that their computation is halted, the bounds are valid, and the leakage is sandwiched between them. Furthermore, under some conditions, our

bounds are “tight”, in that, no better bound exist given the samples so far. In other words, there exist programs that could generate the samples learned so far (are consistent with them) and whose leakage is exactly one of the bounds.

Let $\hat{p}(o_i|h_j)$ be the estimated conditional probability of observable o_i given the high value h_j after some (but not all) symbolic paths are sampled. Specifically, $\hat{p}(o_i|h_j) = \frac{\#(C_i(h_j))}{|\mathcal{D}_n|}$. where $\#(C_i(h_j))$ represents the number of noise values that satisfy the clause C_i for the given h_j based on the collected symbolic paths. Compared to the actual value of $p(o_i|h_j)$ we have:

$$\hat{p}(o_i|h_j) \leq p(o_i|h_j), \quad \forall i, j.$$

This is because the remaining symbolic paths may add to the value of conditional probabilities that are seen so far (but can never subtract from it).

Note that some of the high inputs as well as some observables may not have been part of any samples yet. Let the observables that are seen so far be o_1, \dots, o_k out of o_1, \dots, o_m , where $k \leq m$. The value of m (the size of the space of the observables) may not even be known in advance (before sampling is complete, unlike the size of the space of the high inputs $|\mathcal{D}|$, which is known even before sampling begins). Also, keep in mind that $\hat{p}(o_i|h_j)$ may not yet constitute proper conditional probabilities, that is, we can have: $\sum_{i=1}^k \hat{p}(o_i|h_j) < 1$. This is because for a given h_j not all the observables may be sampled yet, or not even all the contributions to the sampled observables may be accounted for, yet. In this section, as was so far in the paper, the (prior) distribution over the high values is assumed to be uniform. We can also define $\hat{p}(h_j, o_i)$ and $\hat{p}(o_i)$ to respectively be the learned joint probability of (h_j, o_i) , and the probability of output o_i , by symbolic sampling so far. That is:

$$\begin{aligned}\hat{p}(h_j, o_i) &= \frac{1}{|\mathcal{D}|} \hat{p}(o_i|h_j), \\ \hat{p}(o_i) &= \frac{1}{|\mathcal{D}|} \sum_j \hat{p}(o_i|h_j).\end{aligned}$$

Moreover, let $q(h_j)$ be defined as the following:

$$q(h_j) = \frac{1}{|\mathcal{D}|} \left(1 - \sum_i \hat{p}(o_i|h_j) \right). \quad (4)$$

That is, $q(h_j)$ can be thought of as the “unaccounted for” probability for high input h_j that is yet to be learned through future samples. Note that the value of $q(h_j)$ can be measured given the samples so far. Initially, $q(h_j)$ is at $1/|\mathcal{D}|$, and as more paths are sampled, its value reduces to zero. Finally, let Q be the total unexplored probability. That is:

$$Q = \sum_j q(h_j) = 1 - \sum_{i,j} \hat{p}(h_j, o_i) = 1 - \sum_i \hat{p}(o_i). \quad (5)$$

Given this background, we can now present our bounds.

7.2. Upper bounds for side-channel leakage

Proposition 5. *Let $\hat{p}(o|h)$ be the learned values of the (side)-channel of the program resulting from symbolic sampling. Then U_S as given below is a “tight” monotonically decreasing upper-bound for the Shannon leakage:*

$$\begin{aligned}U_S &= \log_2 |\mathcal{D}| - \hat{\mathcal{H}}(h|o), \quad \text{where:} \\ \hat{\mathcal{H}}(h|o) &= - \sum_{i,j} \hat{p}(h_j, o_i) \log_2 \frac{\hat{p}(h_j, o_i)}{\hat{p}(o_i)}.\end{aligned}$$

Similarly, the following is a “tight” monotonically decreasing upper-bound for the Min-Entropy leakage:

$$U_M = \log_2 \left(|\mathcal{D}| \sum_i \max_j \hat{p}(h_j, o_i) + |\mathcal{D}| \cdot Q \right).$$

Before any sampling, the value of the upper-bound (for both Shannon and Min-entropy) is simply $\log_2 |\mathcal{D}|$, i.e., $\mathcal{H}(h)$, which corresponds to a program that completely reveals the value of high.

As mentioned before, by “tightness”, we mean that there exist programs that could produce the observed samples so far (and hence yield measurements $\hat{p}(o|h)$) whose leakage is exactly the above upper-bounds. This tightness is under the assumption that nothing in advance is known about the size of the space of the observables $|\mathcal{O}|$. If $|\mathcal{O}|$ or an upper-bound on it is known in advance (before sampling), then we may no longer have tightness, and our upper-bounds can be improved. For instance, $\log_2 |\mathcal{O}|$ is an upper-bound for (Shannon or Min-entropy) leakage. Suppose it is known (or can be argued) that $|\mathcal{O}| \leq M$ for a constant M where $M < |\mathcal{D}|$. Then we know leakage is less than $\log_2 M$ which is better than the upper-bound in the proposition before any sampling, i.e., $\log_2 |\mathcal{D}|$.

If sampling is done over the symbolic paths obtained by initializing the high input one at a time as we described in Section 5, i.e., scanning the high values concretely while using model counting on the symbolic noise), then this upper-bound can be improved:

Proposition 6. *Suppose the number of possible (side-channel) observables is known to be bound by M . When sampling is done by concrete scanning of the high values and model counting on the symbolic noise, then the following is a (possibly better) monotonically decreasing upper-bound for the Shannon leakage that converges to the real value:*

$$\begin{aligned}U'_S &= \min\{\hat{\mathcal{H}}(o) - Q \log_2 \frac{Q}{M}, \log_2 M\} - \hat{\mathcal{H}}(h, o) \\ &\quad + (1 - Q) \log_2 |\mathcal{D}|, \quad \text{where:} \\ \hat{\mathcal{H}}(o) &= - \sum_i \hat{p}(o_i) \log_2 \hat{p}(o_i), \quad \text{and} \\ \hat{\mathcal{H}}(h, o) &= - \sum_{i,j} \hat{p}(h_j, o_i) \log_2 \hat{p}(h_j, o_i).\end{aligned}$$

7.3. Lower bounds for side-channel leakage

Next, we present our lower-bound:

Proposition 7. Let $\widehat{p}(o|h)$ be the learned values of the (side)-channel of the program resulting from symbolic sampling so far. Then L_S as given below is an any-time lower-bound for the Shannon leakage:

$$L_S = \log_2 |\mathcal{D}| - \widehat{\mathcal{H}}(h|o) + \sum_j q(h_j) \log_2 q(h_j) + (1 - Q) \log_2 (1 - Q)$$

where $\widehat{\mathcal{H}}(h|o)$ is as defined in Proposition 7, and $q(h_j)$ and Q are as defined in (4) and (5), respectively. Moreover, the following is a monotonically non-decreasing lower-bound for the Min-Entropy leakage:

$$L_M = \max \left(\log_2 \left(|\mathcal{D}| \sum_i \max_j \widehat{p}(h_j, o_i) \right), 0 \right)$$

At the beginning of sampling, the value of the leakage’s lower bound for both entropies is zero, which corresponds to the possibility that the program satisfies non-interference. Both lower-bounds converge to the real value by the end of sampling, for Min-entropy, monotonically so.

For a general sampling of both high values and noise, these bounds may not be tight in general. However, we have the following “tightness” result:

Proposition 8. When sampling is done by concrete scanning of the high values and model counting on the symbolic noise, then the lower bounds in Proposition 7 become “tight”.

Again, by tightness, we mean the program under consideration with the observed samples can indeed achieve the lower-bound as its leakage, so it is impossible to improve these lower-bounds.

Note that when using the above per-input sampling, the value of $q(h_j)$ is either zero (for a sampled input), or $p(h) = 1/|\mathcal{D}|$ (for an unexplored input). Hence, the term $\sum_j q(h_j) \log_2 q(h_j)$ in the expression of Shannon’s lower-bound simply becomes $-Q \log_2 |\mathcal{D}|$. When using path sampling with both high and noise symbolic, this term, although computable, is not as straightforward to keep track of. One way to go around this is to use a simpler (albeit looser) lower-bound by noticing that:

$$\sum_j q(h_j) \log_2 q(h_j) \geq Q \log_2 (Q/D)$$

with equality occurring only when $q(h_j) = (\sum_j q(h_j))/|\mathcal{D}| = Q/|\mathcal{D}|$ for all j . Using this inequality gives the overall lower bound as:

$$L'_S = \log_2 |\mathcal{D}| - \widehat{\mathcal{H}}(h|o) + Q \log_2 \frac{Q}{|\mathcal{D}|} + (1 - Q) \log_2 (1 - Q) \quad (6)$$

Hence, compromising on the quality of the lower-bound, we have something that is now easier to compute.

7.4. Confidence Interval

Our bounds implies that the true value of the leakage is within the “error” window of $[L_x, U_x]$, $x \in \{S, M\}$, which goes to zero. The value of this “error” window can be used to stop the sampling once it falls below a desired threshold. Hence, similar to previous work on probabilistic analysis [17] but in the strong notion of this paper, we can define a *confidence interval* $CI_x = [L_x, U_x]$. Our confidence interval is non-probabilistic, that is, the actual leakage is guaranteed to be within it, and, in case of tightness, it cannot be improved.

8. Implementation and Experiments

We implemented the described techniques in the Symbolic PathFinder (SPF) tool, using listeners to monitor the execution of symbolic paths, collect the constraints, perform model counting and sampling. We evaluated them on the following examples, initially provided by DARPA as part of STAC engagements.

- 1) Check Secret, a password-checker that compares a “guess” with an internally stored password, “secret” (see Figure 2), encoded as numbers. The program goes recursively over the elements of an array t of random boolean variables. The “size” refers to the length of array t . Our techniques discovered a timing side-channel caused by the delays in the code.

```

1 boolean checkSecret(int guess, int[] t){
2     return recur(guess, t, t.length - 1);
3 }
4
5 boolean recur(int guess, int[] t, int index){
6     if(index == 0 && t[index] == 1){
7         if(guess <= secret){
8             Thread.sleep(10);
9         }
10        return guess == secret;
11    } else if(t[index] == 1){
12        return recur(guess, t, index - 1);
13    }
14    if(guess <= secret){
15        Thread.sleep(10);
16    }
17    return guess == secret;
18 }
```

Figure 2: The Check Secret example. One of the example programs that we investigate in Section 8.

- 2) CRIME, an instance of the CRIME attack (“Compression Ratio Info-leak Made Easy”) [16]. We analyzed procedure `compress(high.concat(low))`, which implements string compression using the Lempel-Ziv (LZ77) algorithm. We studied both a deterministic and a randomized version: with a probability $p = 3/10$, $k = 1$ bytes are appended to the compressed string before it is sent. The “size” here refers to the the number of characters of high and low strings (i.e., input lengths, which we kept equal for simplicity); Our techniques discovered a space side

- channel, that reveals the secret through the size of the compressed input.
- 3) LawDB, a network service application that manages information about law enforcement personnel. Each employee's data is referenced with a unique employee ID. Standard users are provided operations such as SEARCH and VIEW to manage information about employees except for the ones working on confidential activities. IDs of this particular group of employees are restricted. The requests handling non-confidential records are randomly delayed. In this case, “size” indicates the number of IDs in the database. Our techniques reported a timing channel in the process of handling a SEARCH request that is caused by additional computation, leading to slower response, when there are restricted IDs within the requested search range.
 - 4) Collab, a complex application implementing a network service that provides event scheduling. Users can insert events into the Collab calendar. The events are organized by their ID in a re-balancing tree structure. In addition to regular users, Collab also has special *auditors* that can insert auditing events for other users. It is not possible for regular users to obtain auditing events directly. The application performs logging during the maintenance of the balanced tree. A random number determines how many lines are written to the log file. Our analysis reported both a timing and a space channel that reveals to a user the IDs related to their audits. This is due to the fact that when each node exceeds a certain number of IDs, the node is split into two which results in some logging and which takes additional time.

8.1. Full Exploration of Symbolic Paths

We first evaluated our exact approach. The results are summarized in Table 1 (on page 12). For each example, we report the number of paths (#PC), the Shannon and the Min-Entropy leakages, along with the corresponding execution time. To illustrate the scaling behavior of our approach, we examined our examples for different “size” configurations.

For the CRIME example, we ran experiments on both the deterministic and the randomized versions (columns marked as CRIME and noisy CRIME): the results show that, as expected, the randomized version has smaller leakage for both Shannon and Min-Entropy measures.

8.2. Symbolic Path Sampling

We also experimented with our sampling approach on these examples. Figure 3 plots the lower and upper bounds of Shannon leakage for CRIME as more path samples (shown in percentage on x axis) are analysed. The plot shows how all the bounds converge to the exact leakage. Furthermore, if at any time the exploration is stopped, the real value of leakage is guaranteed to be between the lower and upper-bounds. A similar pattern was observed for all the

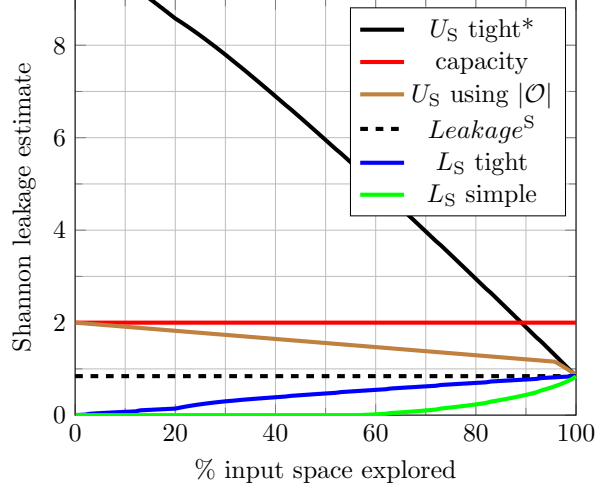


Figure 3: Shannon leakage estimates for CRIME (size 3).

other examples (see e.g. Figure 5 for Check Secret in the Appendix, section F).

We observe that many samples are needed for the tight bound $U_S \text{ tight}^*$ (given by Proposition 5) to get close to the real value. If a bound on the number of observables is known, then a trivial upper-bound on the leakage is the “capacity” bound, i.e., $\log |\mathcal{O}|$. This can be improved using Proposition 6 to an upper-bound that monotonically decreases to the exact leakage (marked as $U_S \text{ using } |\mathcal{O}|$). The $L_S \text{ tight}$ is as provided by Proposition 7, whose tightness comes from Proposition 8. Finally, “ $L_S \text{ simple}$ ” is as per (6), which is of course not as good as the “ $L_S \text{ tight}$ ”.

The plots for Min entropy are illustrated in e.g. Figures 6 (see also 4 in the Appendix, section F). The plots show how all the bounds converge to the exact leakage faster than the Shannon leakage case. Note also that our results can be used for side channel *detection*. For example, if the lower bound for Min entropy leakage is greater than zero, then that means both Min entropy leakage and Shannon leakage are greater than zero, hence we can use the lower bound for Min entropy leakage to *detect* side channels. Thus, even if the bound is not tight, it can be very useful in practice.

8.3. Comparison with “Leakwatch”

We also compared our symbolic sampling with a classical (non-symbolic) Monte-Carlo sampling approach as implemented by “Leakwatch” [10]. We made the comparison using Check Secret; the results are shown in Table 2 (on page 13). The size of t is fixed at 30, and values of the “guess” input, vary from 10 to 9990. The space of the secret, \mathcal{D} , is $\{0 \dots 10000\}$.

“Leakwatch” runs using its default settings. Notice first that, for this program, the leakage reported by the symbolic sampling is the real one (the approach converges quickly); hence we observe that “Leakwatch” wrt symbolic sampling can be very imprecise. In particular in four out of thirteen

| Size | Check Secret | | | CRIME | | noisy CRIME | | LawDB | | Collab |
|----------|--------------|---------|---------|---------|---------|-------------|---------|---------|---------|---------|
| | 100 | 150 | 200 | 3 | 4 | 3 | 4 | 200 | 300 | |
| #PC | 202 | 302 | 402 | 77 | 799 | 154 | 1598 | 615 | 1030 | 2510 |
| Shannon | 0.46757 | 0.46757 | 0.46757 | 0.84290 | 0.92850 | 0.43598 | 0.49412 | 0.77320 | 1.14203 | 0.99712 |
| Time | 99 | 364 | 943 | 4 | 36 | 5 | 49 | 106 | 404 | 472 |
| Min-Ent. | 0.99930 | 0.99930 | 0.99930 | 0.92850 | 1.00000 | 0.76553 | 0.76553 | 3.32193 | 3.32193 | 1.0000 |
| Time | 107 | 412 | 920 | 4 | 37 | 5 | 49 | 158 | 388 | 515 |

TABLE 1: Computation of Shannon and Min-Entropy leakages using symbolic execution and model counting by Barvinok, for our four example case studies. Leakages are measured in bits, times in seconds.

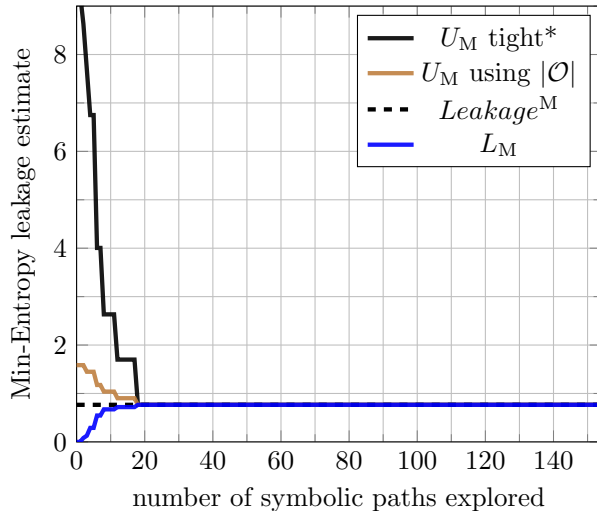


Figure 4: Min-Entropy leakage estimates for CRIME(size 3).

cases “Leakwatch” wrongly report an absence of leakage: these false negatives can have serious security consequences, and could allow an attacker to go unnoticed and, with repeated runs, obtain the whole password. The second observation is the huge difference in analysis time. The symbolic approach takes on average 6 seconds while “Leakwatch” takes on average over 15 minutes.

9. Related Work

Symbolic execution analysis of side channels has been studied in [36], [37]. While these works share a similar symbolic execution platform with our approach, these previous works do not address probabilistic programs or symbolic sampling.

Another approach [24] uses symbolic analysis and Barvinok model counting to quantify information leakage. Compared with our work, that approach is based on a deductive verification system (KeY), and is not fully automated, as it requires user annotations for the KeY proofs. That work applies only to deterministic programs; it translates source code into a logical formula over which projection and model counting are applied. It is not clear how that work could be

applied to probabilistic programs. Furthermore, no sampling is studied in that work.

There have been recent works quantifying leakage using Monte Carlo sampling, e.g. “Leakwatch” [10] and hybrid approaches where sampling is only done under some conditions, e.g. [20]. However these approaches are based on standard sampling techniques, they are not symbolic and hence of a different nature to ours. Also our symbolic framework allows us to prove stronger theoretical guarantees compared to standard sampling techniques.

There is a significant literature on side-channel analysis, for example [3], [8], [9], [14], [25], [26], [32]. Recent works successfully use abstract interpretation for cache side-channels analysis [15], [27], [31]. Our approach differ from these works by using symbolic execution, symbolic sampling and considering probabilistic behavior.

Probabilistic programs are studied in [29], [33] in the context of enforcement [33] and synthesis [29] of privacy policies. Quantification of leakage is relevant to the problem studied in those papers. However compared to those works, our focus is on efficient quantification of leakage of side channels: it is not clear how those works advance on this problem. The case studies from those works are quite small and even the greedy algorithm SynGrd in [29] relies on computing all observables, which can be prohibitively costly in practical terms.

Our lower bounds for Min Entropy leakage are similar to the iterative approach in [4]. However that paper abstracts information systems into channel matrices whereas we develop a concrete program analysis. Another difference with [4] is that we consider both Min Entropy and Shannon leakages.

Also related is the work from [28] which uses symbolic execution and sampling, and proves bounds for Shannon and Min entropy leakage based on sampling. However that work considers standard sampling and applies only to deterministic systems; our bounds are for noisy systems and symbolic sampling. Noise introduces some significant technical challenges; also results on standard sampling do not hold for symbolic sampling, hence these works complement each other. Another work [34] provides bounds on information leakage from a sampling analysis, but it only applies to deterministic systems.

Our symbolic sampling is similar to previous work on probabilistic symbolic execution [18] which was done in

| | | Guess Values | | | | | | | | | | | | |
|-----|------|--------------|--------|--------|--------|--------|--------|--------|--------|--------|--------|--------|--------|--------|
| | | 10 | 100 | 300 | 500 | 1000 | 3000 | 5000 | 8000 | 9000 | 9800 | 9900 | 9980 | 9990 |
| LW | Leak | 0 | 0 | 0.1098 | 0.2008 | 0.3840 | 0.7954 | 0.9155 | 0.6410 | 0.3858 | 0.0633 | 0.0044 | 0 | 0 |
| | Time | 16m29 | 21m9 | 21m22 | 22m1 | 11m22 | 11m8 | 11m54 | 15m1 | 11m35 | 13m27 | 14m46 | 20m23 | 13m16 |
| SPF | Leak | 0.0114 | 0.0806 | 0.1939 | 0.2856 | 0.4676 | 0.8776 | 0.9944 | 0.7145 | 0.4617 | 0.1358 | 0.0761 | 0.0181 | 0.0094 |
| | Time | 6.465 | 6.524 | 6.437 | 6.544 | 6.384 | 5.992 | 6.849 | 6.956 | 7.204 | 7.244 | 6.955 | 6.496 | 7.15 |

TABLE 2: Comparison of Shannon leakage evaluation for the Check Secret example (Figure 2) using “Leakwatch” (LW) and symbolic sampling in SPF. Notice time for Leakwatch is in minutes

the context of checking safety and reliability of software systems. In this paper we provide novel results that allow us to use the information collected with symbolic sampling to compute theoretical lower- and upper- bounds on information leakage.

10. Conclusion

We presented a symbolic approach to computing leakage in noisy side-channels. We also presented a sampling approach to scale up the technique, and provided upper and lower bounds to the leakage. Future work involves investigating model counting techniques for non-linear constraints [5], [6] which will allow us to expand the applicability of the presented techniques to e.g. cryptographic protocols. We also plan to explore distributed versions of our techniques to further increase scalability.

References

- [1] Barvinok library. <http://garage.kotnet.org/~skimo/barvinok/>.
- [2] Giovanni Agosta, Luca Breveglieri, Gerardo Pelosi, and Israel Koren. Countermeasures against branch target buffer attacks. In *Fault Diagnosis and Tolerance in Cryptography, 2007. FDTC 2007. Workshop on*, pages 75–79. IEEE, 2007.
- [3] Dakshi Agrawal, Josyula R. Rao, and Pankaj Rohatgi. Multi-channel Attacks. In Colin D. Walter, Çetin Kaya Koç, and Christof Paar, editors, *Cryptographic Hardware and Embedded Systems - CHES 2003, 5th International Workshop, Cologne, Germany, September 8-10, 2003, Proceedings*, volume 2779 of *Lecture Notes in Computer Science*, pages 2–16. Springer, 2003.
- [4] Miguel E Andrés, Catuscia Palamidessi, Peter Van Rossum, and Geoffrey Smith. Computing the leakage of information-hiding systems. In *TACAS*, pages 373–389. Springer, 2010.
- [5] Mateus Borges, Antonio Filieri, Marcelo d’Amorim, Corina S. Păsăreanu, and Willem Visser. Compositional Solution Space Quantification for Probabilistic Software Analysis. In *Proceedings of the 35th ACM SIGPLAN Conference on Programming Language Design and Implementation, PLDI ’14*, pages 123–132, New York, NY, USA, 2014. ACM.
- [6] Mateus Borges, Quoc-Sang Phan, Antonio Filieri, and Corina S. Păsăreanu. Model-counting approaches for nonlinear numerical constraints. In *NASA Formal Methods: 9th International Symposium, NFM 2017, Moffett Field, CA, USA, May 16-18, 2017, Proceedings*, pages 131–138. Springer International Publishing, 2017.
- [7] Stephen Boyd and Lieven Vandenberghe. *Convex optimization*. Cambridge university press, 2004.
- [8] David Brumley and Dan Boneh. Remote Timing Attacks Are Practical. In *Proceedings of the 12th Conference on USENIX Security Symposium - Volume 12*, SSYM’03, pages 1–1, Berkeley, CA, USA, 2003. USENIX Association.
- [9] Shuo Chen, Rui Wang, XiaoFeng Wang, and Kehuan Zhang. Side-Channel Leaks in Web Applications: A Reality Today, a Challenge Tomorrow. In *Proceedings of the 2010 IEEE Symposium on Security and Privacy, SP ’10*, pages 191–206, Washington, DC, USA, 2010. IEEE Computer Society.
- [10] Tom Chothia, Yusuke Kawamoto, and Chris Novakovic. LeakWatch: Estimating Information Leakage from Java Programs. In *19th European Symposium on Research in Computer Security - Volume 8713*, ESORICS 2014, pages 219–236, New York, NY, USA, 2014. Springer-Verlag New York, Inc.
- [11] Thomas M. Cover and Joy A. Thomas. *Elements of information theory*. Wiley-Interscience, New York, NY, USA, 1991.
- [12] Mark De Berg, Otfried Cheong, Marc Van Kreveld, and Mark Overmars. *Computational Geometry: Introduction*. Springer, 2008.
- [13] Leonardo De Moura and Nikolaj Bjørner. Z3: an efficient SMT solver. In *Proceedings of the 14th international conference on Tools and algorithms for the construction and analysis of systems*, TACAS’08, pages 337–340, Berlin, Heidelberg, 2008. Springer-Verlag.
- [14] Quoc Huy Do, Richard Bubel, and Reiner Hähnle. Exploit Generation for Information Flow Leaks in Object-Oriented Programs. In *ICT Systems Security and Privacy Protection: 30th IFIP TC 11 International Conference, SEC 2015, Hamburg, Germany, May 26-28, 2015, Proceedings*, pages 401–415, Cham, 2015. Springer International Publishing.
- [15] Goran Doychev, Dominik Feld, Boris Köpf, Laurent Mauborgne, and Jan Reineke. CacheAudit: A Tool for the Static Analysis of Cache Side Channels. In *Proceedings of the 22Nd USENIX Conference on Security*, SEC’13, pages 431–446, Berkeley, CA, USA, 2013. USENIX Association.
- [16] Thai Duong and Julian Rizzo. The CRIME attack. In *Presentation at ekoparty Security Conference*, 2012.
- [17] Antonio Filieri, Corina S. Păsăreanu, and Willem Visser. Reliability analysis in symbolic pathfinder. In *Proceedings of the 2013 International Conference on Software Engineering, ICSE ’13*, pages 622–631, Piscataway, NJ, USA, 2013. IEEE Press.
- [18] Antonio Filieri, Corina S. Păsăreanu, Willem Visser, and Jaco Geldenhuys. Statistical Symbolic Execution with Informed Sampling. In *Proceedings of the 22Nd ACM SIGSOFT International Symposium on Foundations of Software Engineering*, FSE 2014, pages 437–448, New York, NY, USA, 2014. ACM.
- [19] Jaco Geldenhuys, Matthew B. Dwyer, and Willem Visser. Probabilistic Symbolic Execution. In *Proceedings of the 2012 International Symposium on Software Testing and Analysis*, ISSTA 2012, pages 166–176, New York, NY, USA, 2012. ACM.
- [20] Yusuke Kawamoto, Fabrizio Biondi, and Axel Legay. Hybrid Statistical Estimation of Mutual Information for Quantifying Information Flow. In *FM*, volume 9995 of *Lecture Notes in Computer Science*, pages 406–425, 2016.

- [21] John Kelsey. Compression and Information Leakage of Plaintext. In *Revised Papers from the 9th International Workshop on Fast Software Encryption*, FSE '02, pages 263–276, London, UK, UK, 2002. Springer-Verlag.
- [22] MHR Khouzani and Pasquale Malacaria. Leakage-Minimal Design: Universality, Limitations, and Applications. In *30th IEEE Computer Security Foundations Symposium (CSF'17)*, 2017.
- [23] James C. King. Symbolic execution and program testing. *Commun. ACM*, 19(7):385–394, July 1976.
- [24] Vladimir Klebanov. Precise quantitative information flow analysisa symbolic approach. *Theoretical Computer Science*, 538:124–139, 2014.
- [25] Paul C. Kocher. Timing Attacks on Implementations of Diffie-Hellman, RSA, DSS, and Other Systems. In *Proceedings of the 16th Annual International Cryptology Conference on Advances in Cryptology*, CRYPTO '96, pages 104–113, London, UK, UK, 1996. Springer-Verlag.
- [26] Boris Köpf and David Basin. An Information-theoretic Model for Adaptive Side-channel Attacks. In *Proceedings of the 14th ACM Conference on Computer and Communications Security*, CCS '07, pages 286–296, New York, NY, USA, 2007. ACM.
- [27] Boris Köpf, Laurent Mauborgne, and Martín Ochoa. Automatic quantification of cache side-channels. In *Proceedings of the 24th international conference on Computer Aided Verification*, CAV'12, pages 564–580, Berlin, Heidelberg, 2012. Springer-Verlag.
- [28] Boris Köpf and Andrey Rybalchenko. Approximation and randomization for quantitative information-flow analysis. In *Computer Security Foundations Symposium (CSF), 2010 23rd IEEE*, pages 3–14. IEEE, 2010.
- [29] Martin Kučera, Petar Tsankov, Timon Gehr, Marco Guarnieri, and Martin Vechev. Synthesis of probabilistic privacy enforcement. In *Proceedings of the 2017 ACM SIGSAC Conference on Computer and Communications Security*, pages 391–408. ACM, 2017.
- [30] Pasquale Malacaria. Algebraic foundations for quantitative information flow. *Mathematical Structures in Computer Science*, 25:404–428, February 2015.
- [31] Heiko Mantel, Alexandra Weber, and Boris Köpf. A Systematic Study of Cache Side Channels Across AES Implementations. In *ESSoS*, volume 10379 of *Lecture Notes in Computer Science*, pages 213–230. Springer, 2017.
- [32] Piotr Mardziel, Mário S. Alvim, Michael W. Hicks, and Michael R. Clarkson. Quantifying Information Flow for Dynamic Secrets. In *2014 IEEE Symposium on Security and Privacy, SP 2014, Berkeley, CA, USA, May 18-21, 2014*, pages 540–555, 2014.
- [33] Piotr Mardziel, Stephen Magill, Michael Hicks, and Mudhakar Srivatsa. Dynamic enforcement of knowledge-based security policies using probabilistic abstract interpretation. *Journal of Computer Security*, 21(4):463–532, 2013.
- [34] Stephen McCamant and Michael D. Ernst. Quantitative information flow as network flow capacity. In *Proceedings of the 2008 ACM SIGPLAN conference on Programming language design and implementation*, PLDI '08, pages 193–205, New York, NY, USA, 2008. ACM.
- [35] David Molnar, Matt Piotrowski, David Schultz, and David Wagner. The program counter security model: Automatic detection and removal of control-flow side channel attacks. In *ICISC*, volume 3935, pages 156–168. Springer, 2005.
- [36] Quoc-Sang Phan, Lucas Bang, Corina S. Păsăreanu, Pasquale Malacaria, and Tevfik Bultan. Synthesis of Adaptive Side-Channel Attacks. In *2017 IEEE 30th Computer Security Foundations Symposium (CSF)*, CSF '17, Washington, DC, USA, August 2017. IEEE Computer Society.
- [37] Corina S. Păsăreanu, Quoc-Sang Phan, and Pasquale Malacaria. Multi-run Side-Channel Analysis Using Symbolic Execution and Max-SMT. In *Proceedings of the 2016 IEEE 29th Computer Security Foundations Symposium*, CSF '16, pages 387–400, Washington, DC, USA, June 2016. IEEE Computer Society.
- [38] Corina S. Păsăreanu, Willem Visser, David Bushnell, Jaco Geldenhuys, Peter Mehlitz, and Neha Runta. Symbolic PathFinder: integrating symbolic execution with model checking for Java bytecode analysis. *Automated Software Engineering*, pages 1–35, 2013.
- [39] Ashay Rane, Calvin Lin, and Mohit Tiwari. Raccoon: Closing Digital Side-channels Through Obfuscated Execution. In *Proceedings of the 24th USENIX Conference on Security Symposium*, SEC'15, pages 431–446, Berkeley, CA, USA, 2015. USENIX Association.
- [40] Geoffrey Smith. On the Foundations of Quantitative Information Flow. In *Proceedings of the 12th International Conference on Foundations of Software Science and Computational Structures*, FOSSACS '09, pages 288–302, Berlin, Heidelberg, 2009. Springer-Verlag.

Appendix A.

Proof of Proposition 5 (Upper-bound)

Proof: We provide the proof for a generalized class of leakages that includes Min-entropy and Shannon as special cases. Assume the expression for the posterior entropy $\mathcal{H}(h|o)$ can be written as follows:

$$\mathcal{H}(h|o) = \eta \left(\sum_{i:p(o_i)>0} p(o_i) F(p(h|o_i)) \right), \quad (7)$$

where η is an $\mathbb{R} \rightarrow \mathbb{R}$ function, and F is a scalar function over the space of probability distributions and one of the following two cases holds:

$$\eta: \text{increasing, and } F: \text{concave}; \quad (8a)$$

$$\eta: \text{decreasing, and } F: \text{convex}. \quad (8b)$$

Shannon entropy follows this structure by choosing η to be the identity function, i.e., $\eta(x) = x$, and $F(p(h|o_i)) = -\sum_j p(h_j|o_i) \log_2(p(h_j|o_i))$, which falls under the case of (8a). Posterior Min-entropy, $-\log_2(\sum_i p(o_i) \max_j(p(h_j|o_i)))$, can be expressed by taking $\eta(x) = -\log_2(x)$ and $F(p(h|o_i)) = \max_j(p(h_j|o_i))$, which complies with case (8b).

We will provide the proof for the case of (8a), the proof for the case of (8b) follows almost identically.

The expression $\sum_{i:p(o_i)>0} p(o_i) F(p(h|o_i))$ in (7) can be cast as a function of $p(h, o)$. Let us denote this dependence explicitly by introducing the function:

$$H(p(h, o)) = \sum_{i:p(o_i)>0} p(o_i) F(p(h|o_i)). \quad (9)$$

The domain of H can be extended beyond legitimate joint probability distributions to include any non-negative $p(h_j, o_i)$, by naturally defining:

$$p(o_i) = \sum_j p(h_j, o_i), \quad p(h|o_i) = (p(h_j|o_i))_j = \left(\frac{p(h_j, o_i)}{p(o_i)} \right)_j$$

By $(p(h_j|o_i))_j$, we mean the $\mathbb{R}^{+|\mathcal{D}|}$ vector whose entries are $p(h_j|o_i)$ and $j = 1, \dots, |\mathcal{D}|$. Note that whenever $p(o_i) >$

0, the vector $p(h|o_i)$ as defined above is still a legitimate probability distribution for h , because each term is non-negative and they add up to one. That is, $p(h_j|o_i) \geq 0 \forall j$, and $\sum_j p(h_j|o_i) = 1$. Hence, $p(h|o_i)$ is still in the domain of F . We prove the proposition using the following lemma:

Lemma 1. *H is “super-additive”, i.e., for any $p_1(h, o)$ and $p_2(h, o)$ on the same space $\mathbb{R}^{+|\mathcal{D}||\mathcal{O}|}$, we have:*

$$H(p_1(h, o) + p_2(h, o)) \geq H(p_1(h, o)) + H(p_2(h, o)).$$

The proof of the lemma is provided separately later, for clarity of exposition. Here, we show how this lemma establishes the upper-bound. Recall that we showed the learned joint probabilities as a result of partial symbolic sampling by $\hat{p}(h, o)$ to distinguish them from the true joint probabilities of the program $p(h, o)$. Let us define $q(h, o)$ as the difference between the true joint probabilities and the learned ones so far. That is, let:

$$q(h, o) := p(h, o) - \hat{p}(h, o)$$

where the difference operation is performed element-wise (i.e., $\forall i, j$). Since any partial symbolic sampling provides an under-estimation of the joint probabilities, we have $\hat{p}(h, o) \leq p(h, o)$, or equivalently $q(h, o) \geq 0$ (element-wise). Now, because we can write $p(h, o) = \hat{p}(h, o) + q(h, o)$, where both $\hat{p}(h, o)$ and $q(h, o)$ are element-wise non-negative, Lemma 1 implies:

$$H(p(h, o)) \geq H(\hat{p}(h, o)) + H(q(h, o)) \quad (10)$$

For the second term in the right hand side, we have:

sub-lemma 1. *For case (8a), if F is further a symmetric function, for any $q(h, o) \geq 0$, we have: $H(q(h, o)) \geq QF(\vec{\delta}_1)$ where $\vec{\delta}_j$ is the degenerate probability distribution that is 1 at h_j and zero at h_k for $k \neq j$, and $Q = \sum_j q(h_j)$.*

For Shannon entropy, the claim of the sub-lemma reduces to $\mathcal{H}_q(h|o) = 0$ where $\mathcal{H}_q(h|o)$ is the familiar posterior entropy where $q(h, o) \geq 0$ is used in place of $p(h, o)$. We provide the proof for the general case:

Proof: Let $\pi = (\pi_1, \dots, \pi_{|\mathcal{D}|})$ be an arbitrary probability distribution over \mathcal{D} . We first show that $F(\pi) \geq F(\vec{\delta}_1)$. This is because π can be written as $\sum_j \pi_j \vec{\delta}_j$. Note that π_j constitute coefficients of a convex combination, because $\pi_j \geq 0$ and $\sum_j \pi_j = 1$. Hence, following concavity of F (Jensen’s inequality) we directly get:

$$F\left(\sum_j \pi_j \vec{\delta}_j\right) \geq \sum_j \pi_j F(\vec{\delta}_j)$$

The left hand side is just $F(\pi)$, and the right hand side, due to the symmetry of F , is equal to $\sum_j \pi_j F(\vec{\delta}_j) = F(\vec{\delta}_1)$. That is, $F(\pi) \geq F(\vec{\delta}_1)$. Now, since for each o_i , $p(h|o_i)$ is a legitimate probability distribution over h , we have:

$$\sum_i q(o_i) F(q(h|o_i)) \geq \sum_i q(o_i) F(\vec{\delta}_1).$$

Since $\sum_i q(o_i) = \sum_j q(h_j) = Q$, the right hand side is $QF(\vec{\delta}_1)$. Hence, $\sum_i q(o_i) F(q(h|o_i)) \geq QF(\vec{\delta}_1)$. \square

Using sub-lemma 1 in (10), noting that for case (8a) η is an increasing $\mathbb{R} \rightarrow \mathbb{R}$ function, we get:

$$\eta(H(p(h, o))) \geq \eta(H(\hat{p}(h, o)) + QF(\vec{\delta}_1))$$

Referring to the definition of H in (9), the left hand side is $\mathcal{H}(h|o)$. Referring to the definition of leakage as $\mathcal{H}(h) - \mathcal{H}(h|o)$, we thus have:

$$\text{Leakage}^{\text{S,M}} = \mathcal{H}(h) - \mathcal{H}(h|o) \leq \mathcal{H}(h) - \eta(H(\hat{p}(h, o)) + QF(\vec{\delta}_1))$$

Note that $\mathcal{H}(h)$ is simply the entropy of the high value, which is known. For instance, for uniform distribution, $\mathcal{H}(h) = \log(|\mathcal{D}|)$. For the case of Shannon entropy, $F(\vec{\delta}_1) = 0$, and hence, the right hand side is $\eta(H(\hat{p}(h, o)))$, which, from (9) and statement of the proposition, is equivalent to $\widehat{\mathcal{H}}(h|o)$. In short, we have:

$$\text{Leakage}^{\text{S,M}} = \mathcal{H}(h) - \mathcal{H}(h|o) \leq \mathcal{H}(h) - \widehat{\mathcal{H}}(h|o)$$

Next, we show that this upper-bound is tight, we construct a (side)-channel that is consistent with the result of partial sampling $\hat{p}(h, o)$ whose leakage is exactly our upper-bound. Let $\widehat{\mathcal{D}}$ and $\widehat{\mathcal{O}}$ respectively be the set of high values and observables that are already encountered in symbolic sampling. Define new extra outputs $\mathcal{O}' = \{o'_1, \dots, o'_{|\mathcal{D}|}\}$ where $\widehat{\mathcal{O}} \cap \mathcal{O}' = \emptyset$. Consider the following channel:

$$\begin{cases} p(o|h) = \hat{p}(o|h) & \forall h \in \widehat{\mathcal{D}}, \forall o \in \widehat{\mathcal{O}} \\ p(o'_j|h_j) = q(h_j) & \forall j = 1, \dots, |\mathcal{D}| \\ p(o|h) = 0 & \text{everywhere else} \end{cases}$$

where $q(h_j) = p(h_j)(1 - \sum_i \hat{p}(o_i|h_j))$, is the total remaining (unexplored) joint probabilities involving h_j , as we already introduced in (4). The leakage for this channel is:

$$\mathcal{H}(h) - \eta\left(\sum_{o \in \widehat{\mathcal{O}}} \hat{p}(o) F(\hat{p}(h|o)) + QF(\vec{\delta}_1)\right)$$

This is exactly the upper-bound we derived, which specifically for Shannon entropy, where $F(\vec{\delta}_1) = 0$, reduces to $\mathcal{H}(h) - \widehat{\mathcal{H}}(h|o)$.

Here, we provide some intuition about this channel: The channel is constructed by “sending” the remaining probability of each high value to a distinct new observable. Intuitively, this is the maximally leaking channel among all possible channels that are consistent with the partially learned channel. In fact, this intuitive explanation is the basis for an alternative proof that uses on Data Processing Inequality (DPI): Any channel can be constructed by concatenating the above channel with another channel, which following DPI leads to a less leaky channel. This shows that the same channel would be the most leaking channel for any form of leakage that satisfies the DPI. Formalizing this line of argument is omitted for brevity.

Finally, to show that $\mathcal{H}(h) - \widehat{\mathcal{H}}(h|o)$ is monotonically decreasing, note that we have so far shown that our upper-bound is the solution to $\max_{p(x,y) \geq \hat{p}(x,y)} \{\mathcal{H}(h) - \mathcal{H}(h|o)\}$. Let $\hat{p}_2(h, o)$ be the updated joint probabilities from $\hat{p}_1(h, o)$

after some more symbolic paths are explored. We have: $\hat{p}_2(h, o) \geq \hat{p}_1(h, o)$ (element-wise). Hence, the solution to $\max_{p(h, o) \geq \hat{p}_2(h, o)} \{\mathcal{H}(h) - \mathcal{H}(h|o)\}$ is a feasible solution of $\max_{p(h, o) \geq \hat{p}_1(h, o)} \{\mathcal{H}(h) - \mathcal{H}(h|o)\}$, and is therefore, lower.

We finish by briefly stating the difference in the proof for (8b) cases, that is, when F is a convex function in probability distributions and η is a decreasing function (as is the case for Min-Entropy). For such cases, Lemma 1 becomes H is “sub-additive”, which implies: $H(\hat{p}(h, o) + q(h, o)) \leq H(\hat{p}(h, o)) + H(q(h, o))$. Moreover, sub-lemma 1 becomes $H(q(h, o)) \leq QF(\vec{\delta}_1)$ for symmetric convex F . Hence, because η is a decreasing function, we have: $\eta(H(p(h, o))) \geq \eta(H(\hat{p}(h, o)) + QF(\vec{\delta}_1))$, which in turn implies: $\mathcal{H}(h) - \mathcal{H}(h|o) \leq \mathcal{H}(h) - \eta(H(\hat{p}(h, o)) + QF(\vec{\delta}_1))$. For Min-entropy, $F(\vec{\delta}_1)$ is simply 1, and $\eta(x) = -\log_2(x)$. Hence, this simplifies to:

$$\text{Leakage}^M \leq \log_2 \left(\frac{\sum_o \max_h \hat{p}(h, o) + Q}{\max_h p(h)} \right)$$

For uniform prior on the high values, the denominator is simply $|\mathcal{D}|$, which leads to the expression in the proposition. The arguments for monotonic convergence and tightness follow as for case (8a). \square

Next, we establish what we left out from the proof of Proposition 5:

Proof of Lemma 1 (super-additivity of H): First, we show that for $\alpha > 0$, $H(\alpha p(h, o)) = \alpha H(p(h, o))$, technically, H is positive homogeneous of degree 1. To see this, note that transforming $p(h, o)$ to $\alpha p(h, o)$ transforms $p(o_i) = \sum_j p(h_j, o_i)$ to $\sum_j \alpha p(h_j, o_i)$, which is $\alpha p(o_i)$. On the other hand, $p(h_j|o_i) = p(h_j, o_i)/p(o_i)$ transforms to $\alpha p(h_j, o_i)/(\alpha p(o_i))$, which, for $\alpha > 0$, is the same as $p(h_j|o_i)$. Hence:

$$\begin{aligned} H(\alpha p(h, o)) &= \sum_{i:\alpha p(o_i)>0} \alpha p(o_i) F(p(h|o_i)) \\ &= \alpha \sum_{i:p(o_i)>0} p(o_i) F(p(h|o_i)) = \alpha H(p(h, o)). \end{aligned}$$

Next, we show that H is concave:

sub-lemma 2. H is concave, i.e., $\forall p_1(h, o)$ and $p_2(h, o)$ on the same space $\mathbb{R}^{+|\mathcal{D}||\mathcal{O}|}$, and $\forall \lambda \in [0, 1]$, we have:

$$H(\lambda p_1(h, o) + (1 - \lambda)p_2(h, o)) \geq \lambda H(p_1(h, o)) + (1 - \lambda)H(p_2(h, o)).$$

Proof: The proof of this claim is similar to that of Proposition 1 in [22] and is included here for completeness. We establish the lemma by expressing H as a composition of a number of transformations that preserve concavity:

- First affine transformation f_i : projection of $p(h, o)$ onto the sub-coordinate where $o = o_i$, that is, the transformation $(p(h_j, o_i))_{i,j} \rightarrow (p(h_j, o_i))_j$. Composition with an affine mapping preserves concavity/convexity.

- Second affine function g_1 : extension of a vector with its summation of elements, i.e., the transformation: $x \rightarrow (x, \sum_j x_j)$.
- Perspective transformation g_2 : Given a function $F : \mathbb{R}^n \rightarrow \mathbb{R}$, consider $g_2 : \mathbb{R}^{n+1} \rightarrow \mathbb{R}$, called *perspective* transformation, defined as follows: $g_2(y, t) = tF(y/t)$ where $\text{dom } g_2 = \{(p, t) \mid p/t \in \text{dom } F, t > 0\}$. Then, if F is concave, so is g_2 [7, Chapter 3.2.6].

Now, we can write

$$\begin{aligned} H(p(h, o)) &= \sum_{i:p(o_i)>0} p(o_i) F(p(h|o_i)) \\ &= \sum_{i:p(o_i)>0} g_2(g_1(f_i(p(h, o)))) . \end{aligned}$$

Hence, H is concave in $p(h, o)$. \square

We are now ready to prove Lemma 1. Consider $p_1(h, o)$ and $p_2(h, o)$ in $\mathbb{R}^{+|\mathcal{D}||\mathcal{O}|}$. Take a $\lambda \in (0, 1)$. Following concavity of H in sub-lemma 2, we can write:

$$\begin{aligned} H\left(\lambda \cdot \frac{p_1(h, o)}{\lambda} + (1 - \lambda) \cdot \frac{p_2(h, o)}{1 - \lambda}\right) \\ \geq \lambda \cdot H\left(\frac{p_1(h, o)}{\lambda}\right) + (1 - \lambda) \cdot H\left(\frac{p_2(h, o)}{1 - \lambda}\right) \end{aligned}$$

The left-hand-side is simply $H(p_1(h, o) + p_2(h, o))$. The right-hand-side, using the positive homogeneity of H , simplifies to $H(p_1(h, o)) + H(p_2(h, o))$. \square

Appendix B.

Proof of Proposition 6 (Improved Upper-bound with the knowledge of a bound on $|\mathcal{O}|$)

Proof: First, $\log_2(|\mathcal{O}|)$ is an upper-bounds for $\mathcal{H}(o)$, which itself is an upper-bound for (Shannon) leakage, since $\text{Leakage} = \mathcal{H}(o) - \mathcal{H}(o|h)$, and $\mathcal{H}(o|h)$, entropy of noise, is always non-negative.

Second, $\mathcal{H}(o) - Q \log_2(Q/|\mathcal{O}|)$ is also an upper-bound for $\mathcal{H}(o)$, because $\mathcal{H}(o) = -\sum_i p(o_i) \log_2 p(o_i)$, and the function $f(t) = -t \log_2 t$ is concave and $f(0) = 0$, so it is super-additive. Recalling $p(o_i) = \hat{p}(o_i) + q(o_i)$, where $p(o_i)$ is the final (real) probability of o_i , and $\hat{p}(o_i)$ is the so far observed probability of o_i (using symbolic sampling) and $q(o_i)$ is the “remaining” probability of o_i (whose value is not yet known). Therefore:

$$-p(o_i) \log_2 p(o_i) \leq -\hat{p}(o_i) \log_2 \hat{p}(o_i) - q(o_i) \log_2 q(o_i)$$

and hence $\mathcal{H}(o) \leq \widehat{\mathcal{H}}(o) - \sum_i q(o_i) \log_2 q(o_i)$. The second term can be bounded above by $-Q \log_2(Q/|\mathcal{O}|)$, which is just the entropy of having a total sum of Q “uniformly distributed” over $|\mathcal{O}|$ elements. This upper-bound starts at $\log_2 |\mathcal{O}|$ and ends at $\mathcal{H}(o)$ with more samples, however, not monotonically so. Hence, a non-increasing upper-bound would be:

$$\mathcal{H}(o) \leq \min\{\widehat{\mathcal{H}}(o) - Q \log_2(Q/|\mathcal{O}|), \log_2(|\mathcal{O}|)\}$$

Third, when doing per input sampling, the observed $\hat{p}(h_j, o_i)$ are at their actual value. Moreover, the remaining terms of $\hat{p}(h_j, o_i) \log_2 \hat{p}(h_j, o_i)$ are all non-positive, so will only reduce the estimate. \square

Appendix C. Proof of Proposition 7 (Lower-bounds)

Proof: First, the proof for Shannon Entropy. Recall that Shannon leakage can be written as:

$$\mathcal{H}(h) - \mathcal{H}(h|o) = \mathcal{H}(h) + \sum_{i,j} p(h_j, o_i) \log_2 \left(\frac{p(h_j, o_i)}{p(o_i)} \right)$$

$p(h, o)$ is the true joint probability. When using symbolic sampling, the explored probability $\hat{p}(h, o)$ so far is an underestimation of the true probability $p(h, o)$. Hence, we can write $p(h, o) = \hat{p}(h, o) + q(h, o)$, where $q(h, o) \geq 0$. Hence, $-\mathcal{H}(h|o)$ can be written as:

$$\sum_{i,j} (\hat{p}(h_j, o_i) + q(h_j, o_i)) \log_2 \left(\frac{\hat{p}(h_j, o_i) + q(h_j, o_i)}{\hat{p}(o_i) + q(o_i)} \right)$$

Consider the function $f(t) = t \log_2(t)$. $f(t)$ is convex and $f(0) = 0$, therefore, it is super-additive. Hence, we have:

$$\begin{aligned} \sum_{i,j} (\hat{p}(h_j, o_i) + q(h_j, o_i)) \log_2 \left(\frac{\hat{p}(h_j, o_i) + q(h_j, o_i)}{\hat{p}(o_i) + q(o_i)} \right) &\geq \\ \sum_{i,j} \hat{p}(h_j, o_i) \log_2 \left(\frac{\hat{p}(h_j, o_i)}{\hat{p}(o_i) + q(o_i)} \right) + \\ \sum_{i,j} q(h_j, o_i) \log_2 \left(\frac{q(h_j, o_i)}{\hat{p}(o_i) + q(o_i)} \right) \end{aligned} \quad (11)$$

In what follows, we find a tight lower-bound for the right hand side (and hence, for $-\mathcal{H}(h|o)$) by casting it as an optimization problem and solve it in closed-form!

$$\begin{aligned} \min_{q(h,o)} \Big\{ & \sum_{i,j} \hat{p}(h_j, o_i) \log_2 \left(\frac{\hat{p}(h_j, o_i)}{\hat{p}(o_i) + q(o_i)} \right) \\ & + \sum_{i,j} q(h_j, o_i) \log_2 \left(\frac{q(h_j, o_i)}{\hat{p}(o_i) + q(o_i)} \right) \Big\} \end{aligned} \quad (12a)$$

subject to:

$$q(h_j, o_i) \geq 0, \forall i, \forall j \quad \& \quad \sum_i q(h_j, o_i) = q(h_j), \forall j \quad (12b)$$

Lemma 2. *The following is a closed-form solution for (12):*

$$q^*(h_j, o_i) = q(h_j) \frac{\hat{p}(o_i)}{\sum_{i'} \hat{p}(o_{i'})} \quad (13)$$

Proof: First, the optimization problem described in (12) is a convex programming. This is because the constraints (12b) are linear (and hence convex), and the objective function (12a) is a convex function in $q(h, o)$. The latter follows as a special case of sub-lemma 2.

To solve a constrained convex optimization problem, the constraints are relaxed by introducing a Lagrange multiplier (dual variable) for each of them (with the right sign) in the objective function and constructing the extended objective function called the Lagrangian, which we will denote by \mathcal{L} . For each inequality constraint $q(h_j, o_i) \geq 0$, we introduce Lagrange multiplier $\lambda_{(h_j, o_i)}$, and for each equality constraint $\sum_i q(h_j, o_i) = q(h_j)$ we introduce μ_{h_j} , as follows:

$$\begin{aligned} \mathcal{L} = & \sum_{i,j} \hat{p}(h_j, o_i) \log_2 \left(\frac{\hat{p}(h_j, o_i)}{\hat{p}(o_i) + q(o_i)} \right) + \\ & \sum_{i,j} q(h_j, o_i) \log_2 \left(\frac{q(h_j, o_i)}{\hat{p}(o_i) + q(o_i)} \right) \\ & - \sum_{i,j} \lambda_{(h_j, o_i)} q(h_j, o_i) + \sum_j \mu_{h_j} \left(q(h_j) - \sum_i q(h_j, o_i) \right) \end{aligned}$$

The μ_{h_j} are free in their sign as they are associated with equality constraints, but we must have:

$$\lambda_{(h_j, o_i)} \geq 0, \quad \forall i, j \quad (14)$$

The optimizer needs to make the first derivatives with respect all variables disappear. In other words, the gradient of the Lagrangian must be zero. After simplification, we get:

$$\begin{aligned} \frac{\partial \mathcal{L}}{\partial q(h_j, o_i)} = 0 \Leftrightarrow \\ \log_2 \left(\frac{q(h_j, o_i)}{\hat{p}(o_i) + q(o_i)} \right) - \lambda_{(h_j, o_i)} - \mu_{h_j} = 0 \end{aligned} \quad (15)$$

Another set of constraints, known as the “complementary slackness” conditions, become the following:

$$\lambda_{(h_j, o_i)} q(h_j, o_i) = 0 \quad (16)$$

The combination of “primal feasibility constraints” (12b), “dual feasibility” (14), “first-order conditions” (15), and “complementary slackness” (16), constitute the Karush-Kuhn-Tucker (KKT) conditions for our problem. In particular, if $q^*(h, o)$, $\lambda_{h,o}^*$ and μ_h^* are found that simultaneously satisfy all the KKT conditions, then $\lambda_{h,o}^*$ is an optimal solution of the primal problem, i.e., the optimization problem in (12). In fact, since all of the constraints (12b) are affine, the KKT conditions are necessary for any optimal solution to satisfy – this is known as “Linearity Constraint Qualification” (LCQ).

Consider the solution candidate given by (13). First of all, the constraints in (15). To see this:

$$\begin{aligned} q(h_j) \frac{\hat{p}(o_i)}{\sum_{i'} \hat{p}(o_{i'})} &\geq 0, \quad \forall i, j \\ \sum_i q(h_j) \frac{\hat{p}(o_i)}{\sum_{i'} \hat{p}(o_{i'})} &= q(h_j) \frac{\sum_i \hat{p}(o_i)}{\sum_{i'} \hat{p}(o_{i'})} = q(h_j), \quad \forall j \end{aligned}$$

Also, whenever $\widehat{p}(o_i) > 0$, we have $q^*(h_j, o_i) > 0$. For such i, j , let $\lambda_{h_j, o_i}^* = 0$ to satisfy (16). Thus, all we need to show can be satisfied is (15). For $q^*(h_j, o_i)$ we have:

$$\begin{aligned}\frac{q^*(h_j, o_i)}{\widehat{p}(o_i) + q^*(o_i)} &= \frac{q(h_j) \frac{\widehat{p}(o_i)}{\sum_{i'} \widehat{p}(o_{i'})}}{\widehat{p}(o_i) + \sum_j q(h_j) \frac{\widehat{p}(o_i)}{\sum_{i'} \widehat{p}(o_{i'})}} \\ &= \frac{\frac{q(h_j)}{1-Q}}{1 + \frac{Q}{1-Q}} = q(h_j)\end{aligned}$$

Hence, choosing $\mu_{h_j}^* = \log_2(q(h_j))$ ensures (15) are also satisfied. Therefore, all KKT conditions are satisfied, and thanks to the sufficiency of KKT for optimality, (13) is an optimal solution of (12). \square

Next, we will replace the minimizing argument given by the lemma into the objective function in (12a) as a lower-bound on $-\mathcal{H}(h|o)$. First, (13) gives:

$$q^*(o_i) = \sum_j q^*(h_j, o_i) = \sum_j q(h_j) \frac{\widehat{p}(o_i)}{\sum_{i'} \widehat{p}(o_{i'})} = \widehat{p}(o_i) \frac{Q}{1-Q}$$

Hence, (12a) becomes:

$$\begin{aligned}&\sum_{i,j} \widehat{p}(h_j, o_i) \log_2 \left(\frac{\widehat{p}(h_j, o_i)}{\widehat{p}(o_i) + \widehat{p}(o_i) \frac{Q}{1-Q}} \right) \\ &\quad + \sum_{i,j} q(h_j) \frac{\widehat{p}(o_i)}{1-Q} \log_2 \left(\frac{q(h_j) \frac{\widehat{p}(o_i)}{1-Q}}{\widehat{p}(o_i) + \widehat{p}(o_i) \frac{Q}{1-Q}} \right) \\ &= \sum_{i,j} \widehat{p}(h_j, o_i) \log_2 \left(\frac{\widehat{p}(h_j, o_i)(1-Q)}{\widehat{p}(o_i)} \right) \\ &\quad + \sum_{i,j} q(h_j) \frac{\widehat{p}(o_i)}{1-Q} \log_2 (q(h_j)) \\ &= \sum_{i,j} \widehat{p}(h_j, o_i) \log_2 \left(\frac{\widehat{p}(h_j, o_i)}{\widehat{p}(o_i)} \right) + \sum_{i,j} \widehat{p}(h_j, o_i) \log_2 (1-Q) \\ &\quad + \sum_{i,j} q(h_j) \frac{\widehat{p}(o_i)}{1-Q} \log_2 (q(h_j)) \\ &= \sum_{i,j} \widehat{p}(h_j, o_i) \log_2 \left(\frac{\widehat{p}(h_j, o_i)}{\widehat{p}(o_i)} \right) + (1-Q) \log_2 (1-Q) \\ &\quad + \sum_j q(h_j) \log_2 (q(h_j))\end{aligned}$$

Referring to the definition of $\widehat{\mathcal{H}}(h|o)$ in Proposition 5, the first term in the last equation above is $-\widehat{\mathcal{H}}(h|o)$. In short, we have shown:

$$-\mathcal{H}(h|o) \geq -\widehat{\mathcal{H}}(h|o) + (1-Q) \log_2 (1-Q) + \sum_j q(h_j) \log_2 q(h_j)$$

which yields:

$$\text{Leakage}^S \geq \mathcal{H}(h) - \widehat{\mathcal{H}}(h|o) + (1-Q) \log_2 (1-Q) + \sum_j q(h_j) \log_2 q(h_j)$$

For uniform prior over high values, $\mathcal{H}(h) = \log_2(|\mathcal{D}|)$. \square

Appendix D.

Proof of Proposition 8 (Tightness of Lower-bounds in Proposition 7 for per-input sampling)

Proof: The proof of tightness for Shannon is immediate when noting that the inequality of (11) is satisfied with equality when for all i, j , either $\widehat{p}(h_j, o_i)$ or $q(h_j, o_i)$ is zero. This is exactly the case when sampling is done by concretely scanning the high value while keeping the noise symbolic. The proof of tightness for Min-Entropy follows by noting that the lower-bound in Proposition (7) is exactly achieved for the legitimate channel described in (13). \square

Appendix E. Computing upper bounds with sampling

Algorithm 5: UpperBoundShannon($P(h, n)$, $\text{obs}(\cdot)$)

```

1  $\mathcal{O} \leftarrow \emptyset$ ,  $Q \leftarrow 1$ ,  $U \leftarrow \log_2(|\mathcal{D}|)$ 
2  $t \leftarrow 0$  /* counter for path samples */
3 while  $Q > 0$  do
4    $t \leftarrow t + 1$ 
5    $PC \leftarrow$  sample a new symbolic path
6    $o \leftarrow \text{obs}(PC)$ 
7    $\pi \leftarrow \frac{\#PC}{|\mathcal{D}| \cdot |\mathcal{D}_n|}$ 
8    $Q \leftarrow Q - \pi$ 
9   if  $o \notin \mathcal{O}$  then /* new observable */
10     $\langle N, \phi_h \rangle \leftarrow \text{BarvH}(PC)$ 
11     $\widehat{p}[o] \leftarrow \pi$ 
12     $u[o] \leftarrow -\pi \cdot \log_2(\#\phi_h)$ 
13    /*  $u[o_i] = p(o_i)\mathcal{H}(h|o_i)$  in  $U = \sum_i u[o_i]$  */
14     $U[t] \leftarrow U[t-1] + u[o]$ 
15     $\mathcal{O} \leftarrow \mathcal{O} \cup o$ 
16     $C[o] \leftarrow PC$ 
17   else /* observable already encountered */
18     $U[t] \leftarrow U[t-1] - u[o]$  /* subtracting
19      the old  $u[o_i] = \widehat{p}(o_i)\widehat{\mathcal{H}}(h|o_i)$  as the only
20      term in  $U = \sum_i u[o_i]$  that changes. */
21     $\widehat{p}[o] \leftarrow \widehat{p}[o] + \pi$ 
22     $C[o] \leftarrow C[o] \vee PC$ 
23     $u[o] \leftarrow 0$  /* computing the new  $u[o]$  */
24    foreach  $\langle N_j, c_j \rangle \in \text{BarvH}(C[o])$  do
25       $p_j \leftarrow \frac{N_j}{|\mathcal{D}| \cdot |\mathcal{D}_n|}$ 
26       $u[o] \leftarrow u[o] + \#c_j \cdot p_j \cdot \log_2 \left( \frac{p_j}{\widehat{p}[o]} \right)$ 
27     $U[t] \leftarrow U[t] + u[o]$ 
28  Prune the symbolic path  $PC$ 
29 return  $U$ 

```

Algorithm 6: UpperBoundMinEnt($P(h, n)$, $\text{obs}(\cdot)$)

```

1  $\mathcal{O} \leftarrow \emptyset, Q \leftarrow 1, U \leftarrow 1$ 
2  $t \leftarrow 0$ 
3 while  $Q > 0$  do
4    $t \leftarrow t + 1$ 
5    $PC \leftarrow \text{sample a new symbolic path}$ 
6    $o \leftarrow \text{obs}(PC)$ 
7    $Q_{\text{new}} \leftarrow Q - \frac{\#PC}{|\mathcal{D}| \cdot |\mathcal{D}_n|}$ 
8   if  $o \notin \mathcal{O}$  then
9      $\langle N, \phi_h \rangle \leftarrow \text{BarvH}(PC)$ 
10     $u[o] \leftarrow \frac{N}{|\mathcal{D}| \cdot |\mathcal{D}_n|}$  /*  $u[o_i] = \max_{h_j} \hat{p}(h_j, o_i)$ 
11      */
12     $U[t] \leftarrow U[t - 1] + u[o] + (Q_{\text{new}} - Q)$ 
13     $\mathcal{O} \leftarrow \mathcal{O} \cup o$ 
14     $C[o] \leftarrow PC$ 
15  else
16     $U[t] \leftarrow U[t - 1] - u[o]$ 
17     $C[o] \leftarrow C[o] \vee PC$ 
18    foreach  $\langle N_j, c_j \rangle \in \text{BarvH}(C[o])$  do
19       $u[o] \leftarrow \max \left\{ u[o], \frac{N_j}{|\mathcal{D}| \cdot |\mathcal{D}_n|} \right\}$ 
20     $U[t] \leftarrow U[t] + u[o] + (Q_{\text{new}} - Q)$ 
21  Prune the symbolic path  $PC$ 
22 return  $\log_2(|\mathcal{D}| \cdot U)$ 

```

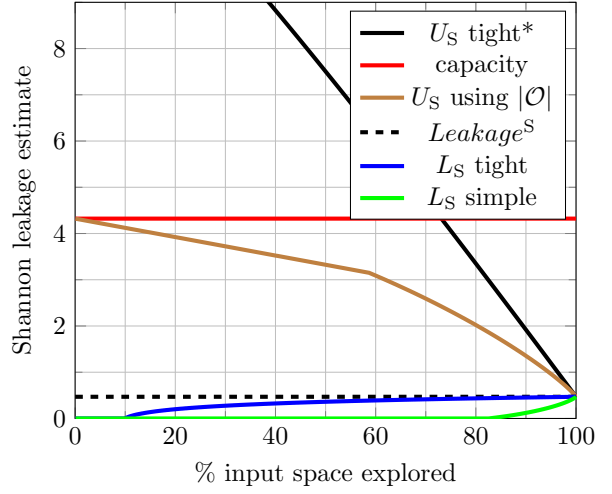


Figure 5: Shannon leakage estimates for Check Secret (guess value is 1000, space of secret is $0, \dots, 10000$ and the size of t is 10).

Appendix F.

Additional material supporting the experiments: results for Check Secret

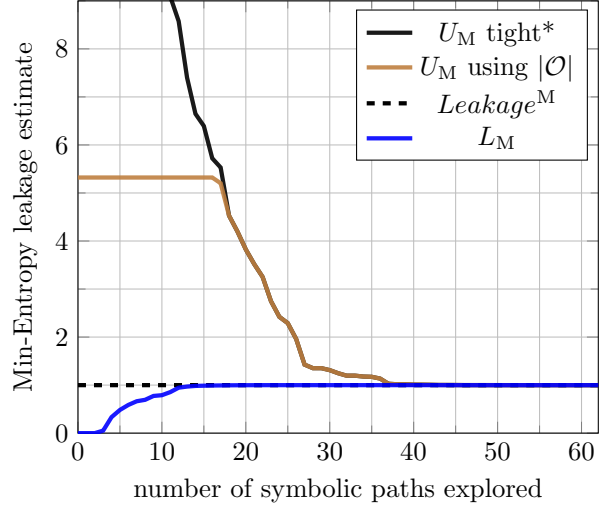


Figure 6: Min-Entropy leakage estimates for Check Secret (guess value is 1000, space of secret is $0, \dots, 10000$ and the size of t is 30).